

UNIVERSIDADE DE LISBOA  
FACULDADE DE CIÊNCIAS  
DEPARTAMENTO DE BIOLOGIA ANIMAL



## **Study of the effects of the culture condition in the permeation of reconstructed human skin**

Mafalda Soares Ferreira Pinto de Pádua

**Mestrado em Biologia Humana e Ambiente**

Dissertação orientada por:  
Professor Doutor Abel Oliva  
Professora Doutora Deodália Dias



**Ciências  
ULisboa**

## **Study of the effects of the culture condition in the permeation of reconstructed human skin**

Mafalda Soares Ferreira Pinto de Pádua

### **Masters in Human Biology and Environment**

This work was held in the Biomolecular Diagnostic Laboratory from ITQB NOVA – Instituto de Tecnologia Química e Biológica António Xavier, an institute of the Universidade NOVA de Lisboa

The bibliographic references were written according to the criteria of Nature

Dissertation mentored by:

Abel Oliva, PhD<sup>1</sup>

Deodália Dias, PhD<sup>2</sup>

<sup>1</sup> Biomolecular Diagnostic Laboratory, Instituto de Tecnologia Química e Biológica (ITQB NOVA) from Universidade Nova de Lisboa, Av. da República, 2780-157 Oeiras, Portugal

<sup>2</sup> Animal Biology Department, Faculdade de Ciências da Universidade de Lisboa, 1749-016 Lisboa, Portugal

# ACKNOWLEDGEMENTS/AGRADECIMENTOS

Ao ITQB NOVA - Instituto de Tecnologia Química e Biológica António Xavier, por me ter disponibilizado as suas instalações e equipamento para realizar o trabalho proposto.

Ao meu orientador, Professor Doutor Abel Oliva, por me ter aceite no seu grupo e me ter permitido fazer investigação numa área que tanto me interessa. Um grande obrigado por toda a paciência, acompanhamento e orientação.

À minha orientadora, Professora Doutora Deodália Dias, pela permanente disponibilidade e apoio demonstrados.

Aos meus colegas de laboratório, Ricardo, Ana Filipa, Patrícia, Vânia e Sara, pela vossa amizade, pela paciência que tiveram para me aturar e por todo o apoio e encorajamento que me deram durante esta jornada.

Ao IGC - Instituto Gulbenkian de Ciência, particularmente à Unidade de Histopatologia pelo processamento das amostras para análise histológica.

Aos meus amigos, por não terem desistido de mim apesar de eu ter estado mais ausente e por todo o apoio e força que me deram.

Por último, à minha família e especialmente aos meus pais, por todo o apoio e encorajamento que me deram durante este percurso.

# SUMÁRIO E PALAVRAS-CHAVE

A indústria farmacêutica e a indústria cosmética estão entre as que mais investem em pesquisa e desenvolvimento, o que leva ao constante aparecimento de novos fármacos e cosméticos. Todos estes produtos, antes de serem introduzidos no mercado, necessitam de passar por uma avaliação criteriosa relativamente à sua eficácia e toxicidade, pois podem provocar efeitos nocivos no organismo humano. Anteriormente, estas avaliações eram realizadas recorrendo à experimentação animal, no entanto com o passar dos anos desenvolveu-se uma consciencialização relativamente ao uso de animais para este fim, o que levou a que restrições legais fossem criadas (em diversos países de todo o mundo) e por conseguinte a uma utilização muito limitada desta prática. Em substituição deste método começaram a desenvolver-se métodos alternativos que permitissem a reprodutibilidade, quantidade e predictibilidade das avaliações.

No que diz respeito aos produtos com aplicação tópica, não só a sua eficácia e toxicidade têm de ser testadas mas também a sua eficiência de penetração. A pele sendo a interface entre o organismo e o seu ambiente externo, constitui uma barreira de proteção contra todas as interferências exteriores e é dividida fundamentalmente em 3 camadas: a hipoderme, a derme e a epiderme, esta última a principal responsável pela função de barreira apresentada por este órgão. A epiderme é a camada mais exterior da pele e é constituída por queratinócitos os quais sofrem um processo contínuo de diferenciação originando um tecido estratificado. Para que o produto aplicado topicamente penetre a pele e tenha o efeito desejado, esta camada tem de ser transposta.

Hoje em dia já existem diversos modelos *in vitro* de pele humana para testar estes produtos, alguns contendo apenas a epiderme, outros apenas a derme e outros ainda contendo ambas as camadas (epiderme e derme). Todos estes modelos se assemelham morfológicamente e bioquimicamente à pele *in vivo*, no entanto ainda não exibem uma adequada propriedade de barreira, evidenciando maiores permeabilidades que a pele nativa. Esta disparidade parece estar relacionada com a camada apical da epiderme - *stratum corneum* - que integra células mortas e achatadas envoltas numa matriz lipídica, onde se observam variações tanto no perfil lipídico como na sua estruturação. Dado verificar-se uma maior permeabilidade nos tecidos *in vitro* do que nos tecidos *in vivo*, sempre que um produto é submetido a avaliações toxicológicas e de eficiência de penetração, extrapolações têm de ser realizadas para fases clínicas o que torna o processo pouco preciso. Surge assim a necessidade de descobrir quais os parâmetros que influenciam a formação da barreira da pele durante a cultura de equivalentes epidérmicos humanos *in vitro*, de forma a gerar um modelo que mais se assemelhe com a epiderme humana nativa, tanto em termos de morfologia como de propriedade barreira.

Assim, este projeto pretendeu produzir equivalentes epidérmicos *in vitro* sob quatro condições distintas, resultantes da alteração independente de quatro fatores relativamente às condições standard de cultura, de forma a avaliar o efeito dessas alterações nos tecidos produzidos e nas suas propriedades de barreira. Para tal, queratinócitos humanos primários isolados foram cultivados em monocamada, cumprindo as regras básicas de cultura celular, e quando estes se encontraram em 4ª passagem foram semeados em insertos com filtro de policarbonato para reconstrução de epidermes *in vitro*, as quais foram obtidas ao fim de onze dias de interface ar-líquido. Após obtenção dos tecidos epidérmicos, foram realizadas análises histológicas de forma a avaliar as características morfológicas e ensaios de permeabilidade a três fármacos de diferentes polaridades (caféina, hidrocortisona e testosterona) em células de difusão de Franz para avaliar as propriedades de barreira. Os resultados das análises histológicas foram avaliados por observação microscópica enquanto que os resultados dos ensaios de permeabilidade foram avaliados

por leitura espectrofotométrica, a partir da qual se obteve a quantidade de fármaco permeada pelo tecido ao longo do ensaio, que permitiu calcular o seu fluxo.

As quatro alterações testadas, que foram implementadas durante a fase de exposição da cultura à interface ar-líquido, foram: (1) o aumento da disponibilidade de factores de autocrinos e homocrinos; (2) o aumento da disponibilidade de nutrientes via suplementação do meio de cultura com FBS; (3) a diminuição da temperatura de incubação; (4) o aumento da disponibilidade de oxigénio. A alteração relativa aos factores autocrinos e homocrinos resultou da dedução de que as células dispunham de pouco tempo em contacto com os factores de sinalização produzidos por elas. Como tal, primeiramente variou-se o período de renovação dos meios de modo a avaliar qual o período ótimo entre renovações consecutivas e posteriormente cultivou-se tecido epidérmico com um período entre renovações estendido de forma a aumentar a sua exposição aos factores. A alteração relativa à suplementação do meio de cultura com FBS adveio de resultados contraditórios descritos na bibliografia, em que certos estudos descrevem o FBS como sendo benéfico para o desenvolvimento da cultura, enquanto que outros descrevem-no como prejudicial. Como tal, realizou-se uma cultura em que este suplemento foi adicionado, numa concentração de 10%, ao meio de cultura de forma a avaliar os seus efeitos. A alteração da temperatura derivou da constatação de que os queratinócitos que integram a epiderme crescem naturalmente a 32 °C, temperatura registada à superfície da pele, contrariamente à maioria das células que crescem à temperatura fisiológica humana (37 °C). Como tal, inicialmente avaliou-se o impacto da redução da temperatura, para 32 °C, no período de desenvolvimento dos queratinócitos e posteriormente desenvolveu-se uma cultura sob essas mesmas condições de forma a avaliar o efeito da temperatura natural na formação da epiderme. A alteração da disponibilidade de oxigénio surgiu de um resultado proveniente de um estudo realizado anteriormente no laboratório, o qual indicava que as células estavam sob condições limitantes de oxigénio. Como tal, aumentou-se a superfície de contacto entre o meio e a atmosfera de forma a permitir a solubilização de mais oxigénio no meio que nutre as células.

Os resultados obtidos em cada alteração foram comparados com os resultados obtidos em equivalentes epidérmicos humanos produzidos *in vitro* segundo o protocolo adoptado como standard. Verificou-se que à excepção da cultura suplementada com FBS, todas as alterações geraram tecidos com a propriedade de barreira melhorada, ou seja, com uma permeabilidade mais reduzida. Quando a exposição aos factores autocrinos e homocrinos foi aumentada, assim como quando a temperatura de incubação foi diminuída, foram produzidos tecidos bem diferenciados e com uma espessura média superior à apresentada pelos tecidos epidérmicos cultivados em condições standard. Consequentemente, a permeabilidade destes tecidos à cafeína e à testosterona melhorou significativamente ( $p < 0.05$ ), contudo não alterou a permeabilidade à hidro cortisona ( $p > 0.05$ ). Quando se aumentou a disponibilidade de oxigénio produziram-se tecidos bem diferenciados, mas com uma espessura média bastante próxima à apresentada pelos tecidos epidérmicos cultivados em condições standard. Consequentemente, a permeabilidade destes tecidos à cafeína e à hidro cortisona não mostraram alterações significativas ( $p > 0.05$ ), contudo apresentaram melhorias significativas na permeabilidade à testosterona ( $p < 0.05$ ). No que diz respeito ao aumento da disponibilidade de nutrientes via suplementação do meio de cultura com FBS, constatou-se que o tecido produzido era pouco diferenciado e estratificado além de pouco compacto. Isto refletiu-se na sua permeabilidade, a qual piorou significativamente relativamente à cafeína e à hidro cortisona ( $p < 0.05$ ), apesar de não ter alterado significativamente a permeabilidade à testosterona ( $p > 0.05$ ).

Estes resultados parecem promissores para o desenvolvimento de um protocolo otimizado, porém outros testes complementares à análise histológica e aos ensaios de permeabilidade deveriam ser realizados para uma melhor compreensão do impacto das alterações nos tecidos produzidos.

Assim, este trabalho contribui para a percepção de como estes parâmetros podem ser variados para produzir um equivalente epidérmico humano *in vitro* mais semelhante à epiderme humana nativa. No entanto, é claro que mais estudos são necessários, pois os valores de permeabilidade ainda estão longe dos observados *in vivo*.

**Palavras-Chave:** Epiderme; equivalentes epidérmicos humanos *in vitro*; permeabilidade; função de barreira

# ABSTRACT AND KEYWORDS

The skin is the interface between the organism and the external environment, and its outermost layer - epidermis - is the major responsible for the barrier function of this organ. As such, epidermis is a crucial obstacle to be overcome by any substance intended to penetrate the skin.

Cosmetic and pharmaceutical products for topical administration, prior to their placement in the market, are evaluated as to their safety and efficacy as well as penetration efficiency. Previously these tests were performed using animal experimentation. However due to legal demands, this use was discontinued and replaced by *in vitro* human skin equivalents. Although the *in vitro* epidermal models currently produced resemble the morphological and biochemical characteristics of the human epidermis, their barrier function is still reduced when compared to *in vivo* skin, evidencing higher permeability values which require extrapolation to clinical stages. Thus, it is necessary to discover the parameters that influence the skin barrier formation during epidermal tissue culture, in order to generate an *in vitro* model that better resembles the *in vivo* human epidermis.

This work aimed to produce human epidermal equivalents under four different conditions in order to evaluate the effect of these alterations on the cultured tissue barrier function. The four studied conditions were: increased availability of cellular growth factors; increased availability of nutrients via FBS supplementation; lowered incubation temperature; increased availability of oxygen. Subsequently their morphology was assessed by histological analysis and their permeability by diffusion studies in Franz diffusion cells using three model drugs with different polarities (caffeine, hydrocortisone and testosterone).

Out of the four conditions tested, the ones related to cellular growth factors, temperature and oxygen have shown to produce well stratified and differentiated tissues containing all the expected *strata*. Additionally, these tissues have evidenced statistically significant improvements in reducing permeability. The same was not true for FBS medium supplementation which produced tissues that were poorly consistent and differentiated without a well-defined stratification. These tissues evidenced statistically significant worsening in reducing permeability.

This work provides a preliminary insight into how these parameters can be adjusted to produce an *in vitro* human epidermal equivalent that better resembles the *in vivo* human epidermis. Although it is clear that further study is needed as permeability values are still far from those observed *in vivo*.

**Keywords:** epidermis; *in vitro* human epidermal equivalents; barrier function; permeability

# INDEX

ACKNOWLEDGEMENTS/AGRADECIMENTOS .....	II
SUMÁRIO E PALAVRAS-CHAVE.....	III
ABSTRACT AND KEYWORDS .....	VI
INDEX .....	VII
TABLE INDEX.....	IX
FIGURE INDEX .....	X
NOMENCLATURE .....	XII
INTRODUCTION .....	1
1.1. The Human Skin .....	2
1.1.1. Skin structure.....	2
1.1.2. Permeation routes through skin .....	5
1.2. <i>In vitro</i> Human Skin Models .....	7
1.2.1. Human Epidermal models .....	8
1.2.2. Attempts to improve the <i>in vitro</i> epidermal models .....	9
1.3. New attempts to improve the <i>in vitro</i> epidermal models.....	10
1.3.1. Conditions intended to screen .....	10
1.3.2. Franz diffusion cells .....	11
MATERIALS AND METHODS .....	14
2.1. Cell culturing and <i>in vitro</i> reconstruction of human epidermis .....	14
2.1.1. Preparation of solutions.....	14
2.1.2. Monolayer cell culturing .....	15
2.1.3. Reconstruction of human epidermis .....	16



2.2. Assessment of epidermis' permeability.....	18
2.2.1. Testosterone solubility .....	18
2.2.2. Diffusion studies.....	19
2.2.3. Samples analysis.....	19
2.2.4. Data analysis.....	20
2.3. Histological analysis of reconstructed epidermis .....	21
RESULTS AND DISCUSSION .....	22
3.1. Testosterone Solubility .....	22
3.2. <i>In vitro</i> reconstruction of human epidermis and assessment of its permeability.....	23
3.3. Attempts to improve the barrier properties of <i>in vitro</i> epidermis.....	28
3.3.1. Availability of autocrine and homocrine factors .....	28
3.3.2. Nutrients availability .....	31
3.3.3. Temperature.....	34
3.3.4. Oxygen availability .....	38
CONCLUSION .....	42
REFERENCES.....	44
APPENDIX A .....	50

# TABLE INDEX

<b>Table 2.1</b> - Variations assessed in the culture conditions. ....	17
<b>Table 3.1</b> - Values obtained for the permeability parameters of the different model drugs in the reconstructed human epidermis (RHE) grown under standard conditions (average $\pm$ SD). ....	25
<b>Table 3.2</b> - Values obtained from bibliographic references for the permeability parameters of the different model drugs in commercial models and in human cadaver skin (average $\pm$ SD). ....	26
<b>Table 3.3</b> - Comparison of the values obtained for the permeability parameters of the different model drugs in the reconstructed human epidermis (RHE) grown in culture medium renewed only every 72 hours and in the reconstructed human epidermis (RHE) grown under standard conditions (average $\pm$ SD). ....	29
<b>Table 3.4</b> - Comparison of the values obtained for the permeability parameters of the different model drugs in the reconstructed human epidermis (RHE) grown in culture medium additionally supplemented with 10% FBS and in the reconstructed human epidermis (RHE) grown under standard conditions (average $\pm$ SD). ....	32
<b>Table 3.5</b> - Comparison of the values obtained for the permeability parameters of the different model drugs in the reconstructed human epidermis (RHE) grown at 32 °C for 22 days and in the reconstructed human epidermis (RHE) grown under standard conditions (average $\pm$ SD). ....	36
<b>Table 3.6</b> - Comparison of the values obtained for the permeability parameters of the different model drugs in the reconstructed human epidermis (RHE) grown in petri dishes and in the reconstructed human epidermis (RHE) grown under standard conditions (average $\pm$ SD). ....	39

# FIGURE INDEX

<b>Figure 1.1</b> - Structure of human skin: The 3 different skin layers (epidermis, dermis and hypodermis, from the outer to the innermost layer, respectively) and their accessory structures. ....	2
<b>Figure 1.2</b> - Epidermal differentiation: The different <i>strata</i> that compose epidermis and their main constituents. ....	3
<b>Figure 1.3</b> - Pathways for permeation through the skin: Molecules diffuse either through the intercellular spaces, through keratinocytes or even through skin appendages. ....	6
<b>Figure 1.4</b> - Crucial steps for the reconstruction of epidermal equivalents. ....	9
<b>Figure 1.5</b> - Three main types of diffusion cells: (A, C) Franz-type diffusion cell and Flow-through diffusion cell, respectively, both mainly used for <i>in vitro</i> percutaneous absorption studies; (B) Side-by-side diffusion cell, mainly used for evaluation of skin immersed conditions. ....	12
<b>Figure 2.1</b> - Monitorization of culture growth: Keratinocytes covering 10% (I, II); 20% (III, IV); 40% (V, VI); 60% (VII, VIII); 80% (IX, X) of t-flask surface. Magnifications: 40x (I, III, V, VII, IX); 200x (II, IV, VI, VIII, X). ....	16
<b>Figure 2.2</b> - Diffusion studies equipment: Hand-blown Franz-type diffusion cell (A) and the complete experimental apparatus (B), in which 5 diffusion cells are dipped in a thermostatic bath maintained at a constant temperature. ....	18
<b>Figure 3.1</b> - Unsolubilized testosterone, by visual inspection, in the different solutions after 24 hours of agitation: (A) PBS solution with a lot of testosterone non-solubilized, (B) PBS + 1% Tween®20 with some testosterone non-solubilized and (C) PBS + 1% Brij®58 with almost none testosterone non-solubilized. ....	22
<b>Figure 3.2</b> - Testosterone solubility profile over 24 hours of agitation in the different solutions. ....	23
<b>Figure 3.3</b> - Evolution of epidermis thickness when cultivated at 37 °C, during the days surrounding the standard air-liquid interface period (n = 6, average ± SD). ....	24
<b>Figure 3.4</b> - Fully differentiated epidermis with the <i>strata</i> that compose epidermis pointed out (approx. 54 µm thick). Magnification 400x. ....	24
<b>Figure 3.5</b> - Morphology of the reconstructed human epidermis grown under standard conditions, after 12 days at air-liquid interface (approx. 52 µm thick). Magnification 400x. ....	25
<b>Figure 3.6</b> - Caffeine permeability profile over 24 hours of sampling in reconstructed human epidermis (RHE) grown under standard conditions (n = 5, average ± SD). ....	26
<b>Figure 3.7</b> - Hydrocortisone permeability profile over 24 hours of sampling in reconstructed human epidermis (RHE) grown under standard conditions (n = 4, average ± SD). ....	27
<b>Figure 3.8</b> - Testosterone permeability profile over 24 hours of sampling in reconstructed human epidermis (RHE) grown under standard conditions (n = 4, average ± SD). ....	27
<b>Figure 3.9</b> - Morphology of (A) the reconstructed human epidermis grown in culture medium renewed every 72 hours (approx. 60 µm thick) and (B) the reconstructed human epidermis grown in culture	

medium renewed every 96 hours (approx. 41 $\mu\text{m}$ thick), after 12 days at air-liquid interface. Magnification 400x. ....	28
<b>Figure 3.10</b> - Morphology of the reconstructed human epidermis grown in culture medium renewed only every 72 hours, after 12 days at air-liquid interface (approx. 65 $\mu\text{m}$ thick). Magnification 400x. ..	29
<b>Figure 3.11</b> - Caffeine permeability profile over 24 hours of sampling in reconstructed human epidermis (RHE) grown in culture medium renewed only every 72 hours. (n = 5, average $\pm$ SD). ....	30
<b>Figure 3.12</b> - Hydrocortisone permeability profile over 24 hours of sampling in reconstructed human epidermis (RHE) grown in culture medium renewed only every 72 hours. (n = 5, average $\pm$ SD). ....	30
<b>Figure 3.13</b> - Testosterone permeability profile over 24 hours of sampling in reconstructed human epidermis (RHE) grown in culture medium renewed only every 72 hours. (n = 5, average $\pm$ SD). ....	31
<b>Figure 3.14</b> - Morphology of the reconstructed human epidermis grown in culture medium additionally supplemented with 10% FBS, after 12 days at air-liquid interface (approx. 40 $\mu\text{m}$ thick). Magnification 400x. ....	32
<b>Figure 3.15</b> - Caffeine permeability profile over 24 hours of sampling in reconstructed human epidermis (RHE) grown in culture medium additionally supplemented with 10% FBS. (n = 5, average $\pm$ SD). ....	33
<b>Figure 3.16</b> - Hydrocortisone permeability profile over 24 hours of sampling in reconstructed human epidermis (RHE) grown in culture medium additionally supplemented with 10% FBS. (n = 5, average $\pm$ SD). ....	33
<b>Figure 3.17</b> - Testosterone permeability profile over 24 hours of sampling in reconstructed human epidermis (RHE) grown in culture medium additionally supplemented with 10% FBS. (n = 5, average $\pm$ SD). ....	34
<b>Figure 3.18</b> - Evolution of epidermis thickness when cultivated at 32 $^{\circ}\text{C}$ , starting on the 13 <sup>th</sup> day of standard air-liquid interface period and ending on the 30 <sup>th</sup> day of air-liquid interface (n = 6, average $\pm$ SD). ....	35
<b>Figure 3.19</b> - Morphology of the reconstructed human epidermis grown at 32 $^{\circ}\text{C}$ , after 22 days at air-liquid interface (approx. 86 $\mu\text{m}$ thick). Magnification 400x. ....	36
<b>Figure 3.20</b> - Caffeine permeability profile over 24 hours of sampling in reconstructed human epidermis (RHE) grown at 32 $^{\circ}\text{C}$ for 21 days. (n = 5, average $\pm$ SD). ....	37
<b>Figure 3.21</b> - Hydrocortisone permeability profile over 24 hours of sampling in reconstructed human epidermis (RHE) grown at 32 $^{\circ}\text{C}$ for 22 days. (n = 4, average $\pm$ SD). ....	37
<b>Figure 3.22</b> - Testosterone permeability profile over 24 hours of sampling in reconstructed human epidermis (RHE) grown at 32 $^{\circ}\text{C}$ for 23 days. (n = 5, average $\pm$ SD). ....	38
<b>Figure 3.23</b> - Morphology of the reconstructed human epidermis grown in petri dishes, after 12 days at air-liquid interface (approx. 56 $\mu\text{m}$ thick). Magnification 400x. ....	39
<b>Figure 3.24</b> - Caffeine permeability profile over 24 hours of sampling in reconstructed human epidermis (RHE) grown in petri dishes. (n = 5, average $\pm$ SD). ....	40
<b>Figure 3.25</b> - Hydrocortisone permeability profile over 24 hours of sampling in reconstructed human epidermis (RHE) grown in petri dishes. (n = 5, average $\pm$ SD). ....	40
<b>Figure 3.26</b> - Testosterone permeability profile over 24 hours of sampling in reconstructed human epidermis (RHE) grown in petri dishes. (n = 5, average $\pm$ SD). ....	41

# NOMENCLATURE

% – percent

$\lambda$  – Wavelength

$\mu$  (unit prefix) – micro

2D – Two-Dimensional

3D – Three-Dimensional

BMI – Body-Mass Index

Brij®58 – Polyoxyethylene-20-cetyl ether

BSA – Bovine Serum Albumin

°C – degree Celsius (SI Unit)

c (unit prefix) – centi

CaCl<sub>2</sub> – Calcium Chloride

CO<sub>2</sub> – Carbon Dioxide

Da – Dalton

DFBS – Dialysed Fetal Bovine Serum

DMSO – Dimethyl sulfoxide

ECVAM – European Center for the Validation of Alternative Methods

EDTA – Ethylenediaminetetraacetic acid

EU – European Union

FBS – Fetal Bovine Serum

FFAs – Free Fatty Acids

g – force of gravity

g – gram (SI Unit)

h – hour

H & E – Hematoxylin and Eosin

H<sub>2</sub>O – Water

HEKn – neonatal Human Epidermal Keratinocytes

HKGS – Human Keratinocyte Growth Supplement

HU – Histopathology Unit

IGC – Instituto Gulbenkian de Ciência

Igepal® – Octylphenoxy poly-ethyleneoxy-ethanol

ITQB – Instituto de Tecnologia Química e Biológica

$J_{\text{max}}$  – Maximum Flux  
 KCl – Potassium Chloride  
 KGF – Keratinocyte Growth Factor  
 $\text{KH}_2\text{PO}_4$  – Monopotassium phosphate  
 L – Liter  
 $\log P$  – Octanol-water partition coefficient  
 m – meter (SI Unit)  
 M – Molar (SI Unit)  
 m (unit prefix) – milli  
 n (unit prefix) – nano  
 $\text{N}_2$  – Nitrogen  
 $\text{Na}_2\text{HPO}_4$  – Disodium Hydrogen Phosphate  
 NaCl – Sodium Chloride  
 $\text{O}_2$  – Oxygen  
 OECD – Organization for Economic Co-operation and Development  
 OR – Oregon  
 PBS – Phosphate-buffered saline  
 PG – Propylene Glycol  
 pH – potential of Hydrogen  
 $Q_{24}$  – Cumulative Corrected Amount of compound crossed per unit of area of skin in 24 hours  
 RH – Relative Humidity  
 RHE – Reconstructed Human Epidermis  
 SB – *Stratum Basale*  
 SC – *Stratum Corneum*  
 SD – Standard Deviation  
 SG – *Stratum Granulosum*  
 SL – *Stratum Lucidum*  
 SS – *Stratum Spinosum*  
 Tween®20 – Polyoxyethylenesorbitan monolaurate  
 USA – United States of America  
 UV – Ultraviolet  
 UV-Vis – Ultraviolet and Visible

# CHAPTER 1

## INTRODUCTION

Healthcare industry is among the industries that most invest in research and development, which allows large pharmaceutical, medical and biotechnological innovations to emerge in short periods of time. Any new drug or biologic developed in this industry, whether of topical, enteral or parenteral administration, must be tested as to its toxicity and safety for the organism, prior to their placement in the market. Previously, these studies relied on animal experimentation, however over the years a consciousness regarding the use of animals began to arise and non-animal methods began to be prospected<sup>1-3</sup>.

In 1959, a major step towards the awareness of animal testing was taken with the publication of *The Principles of Humane Experimental Technique* by William Russell and Rex Burch, which brought to the attention of the scientific community three simple principles (“3 Rs”) that should be taken into account when animal experimentation was considered. These principles encouraged researchers to reduce the number of animals used in an experiment to the minimum necessary, prioritizing the use of animals with lower neurological development; to refine the conditions to which animals were exposed so that the pain and distress caused on the animals were minimal; and to replace the use of animals with alternative non-animal methods whenever possible. The above-mentioned concepts gained such a recognition that were incorporated into the EU Directive 86/609 in 1986 and reinforced in several legislations all over the world<sup>3-5</sup>.

Despite Russel and Burch’s effort to raise awareness on this subject, the number of animals used in laboratory practices continued to increase, so in 2013 European Parliament and European Council banned the animal testing for toxicity evaluation of cosmetic ingredients in Europe (Directive 2003/15/EC). As in Europe, also in other countries such as Japan and United States of America (USA) legislations limiting animal testing appeared<sup>4,6</sup>.

Since legal restrictions on animal experimentation were imposed, non-animal alternative methods were taken more seriously and implemented on several basic and applied research studies. Considering that a large percentage of the animals used for scientific purposes in the European Union were used in toxicological and other safety assessments (80%, according to data from 2005<sup>5</sup>), various methods have been proposed as alternatives in drug testing and toxicological screenings, which allow the reproducibility, quantity and predictability required in these evaluations. Included on these methods are the cell and tissue cultures, namely of human origin<sup>2,3,5</sup>.

Regarding topically administered drugs, *in vitro* engineered human skin models were recognized as the best alternative to the use of animal models. Even though *ex vivo* human skin samples, mainly obtained either from cadavers or biopsies, were for a while also a plausible alternative as it successfully replicated *in vivo* skin properties, its limited availability as well as poor reproducibility due to variation on skin properties depending on factors such as donor’s ethnicity, age, gender, skin type, body-mass index (BMI) and lifestyle, caused this approach to be discarded. Thus, increased efforts were devoted to the

development of consistent three-dimensional (3D) human skin equivalents that allowed the performance of release-rate estimates besides toxicity assessments<sup>6-9</sup>.

Although these alternative approaches are currently of great value on helping to explain and predict several *in vivo* behaviors, the existing models are still not able to fully portray all the biological features and processes. In order to improve these models and make better predictions of human biological responses, more commitment on the part of the scientific community must be directed towards the optimization of cell cultures, so that better and more accurate models emerge<sup>2,4,5,10</sup>.

## 1.1. THE HUMAN SKIN

The skin is the largest organ of the human body and the first line of defense against the innumerable external aggressions that it can suffer, functioning as a protective interface between the organism and its external environment. This organ, along with the accessory structures, such as hair, glands and nails, form the integumentary system. In order to carry out its numerous functions, whether of protection, regulation, metabolic, immune and nervous, the skin presents a massive complexity, being constituted by a multiplicity of different types of cells, along with accessory structures, that interact with each other<sup>7-9,11-14</sup>.

### 1.1.1. SKIN STRUCTURE

The skin is divided fundamentally into 3 different layers: hypodermis, dermis and epidermis (Figure 1.1).

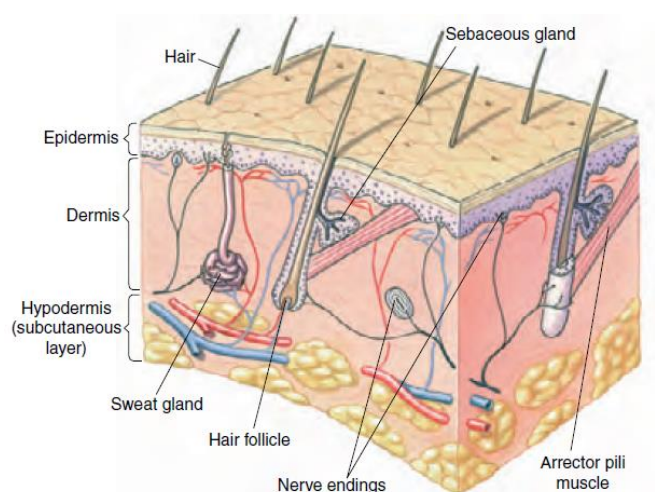


**Figure 1.1** - Structure of human skin: The 3 different skin layers (epidermis, dermis and hypodermis, from the outer to the innermost layer, respectively) and their accessory structures. (Adapted from<sup>13</sup>)

Hypodermis is the innermost layer of the integumentary system and is essentially composed by adipocytes although containing some fibroblasts and macrophages. Despite working as a connection between the skin and the muscles or bones and as a supplier of blood vessels and nerves to the other layers of the skin, its major functions are as thermal insulator, nutritional storage and shock absorber<sup>9,11,14,15</sup>.

Dermis, accounting for around 90 % of the weight of the skin, is the middle layer of the integumentary system, being delimited inferiorly by the hypodermis and superiorly by the epidermis. This layer consists of connective tissue, where collagen, elastin and glycosaminoglycans, collectively, comprise



the extracellular matrix, produced by the primary cell type of dermis, fibroblasts. Its main role is to provide foundation, structural strength and elasticity to the system. Blood and lymph vessels are abundant in this skin region, having the responsibility of removing metabolites and supplying nutrients both to dermis and epidermis, since the last represents an avascular structure. The majority of skin appendages, such as hair follicles, sebaceous glands and sweat glands, as well as nerve endings are anchored to dermis<sup>9,11,12,14,15</sup>.

Basement Membrane Zone or Dermal-Epidermal Junction is the acellular band between the epidermis and dermis and is mainly composed by a laminin/collagen IV scaffold secreted by both its adjacent layers. This junction's functions are to anchor the epidermis to dermis, as well as regulate the molecular and cellular exchanges between the two skin layers and provide some structural and mechanical support to epidermis<sup>11,16</sup>.

Epidermis is the outermost layer of the skin and the main responsible for the barrier property of this organ. Among its functions is the protection of the organism from mechanical injuries, microorganisms, chemicals, and radiation present in the environment, as well as the regulation of water and heat losses and production of vitamin D. The stratified squamous epithelium that characterizes this skin layer includes several types of cells, such as melanocytes, Langerhans cells and Merkel cells, however its major constituent are keratinocytes (90%). Keratinocytes are a type of cells named after the structural protein mixture that they produce called keratins, classified as intermediate filament, which hardens them, as well as the hair and nails, and provides them the strength needed to resist abrasion and to accomplish the functions of protection associated to this outermost skin layer. This system of production and accumulation of keratin by keratinocytes is called keratinization or cornification and is part of the process of cytodifferentiation, which the keratinocytes undergo to originate a stratified tissue. During this differentiation process, as new keratinocytes arise from mitosis in the deepest layer of epidermis, older ones are pushed towards the surface, continuously changing their shapes as well as chemical composition, until they slough off. In addition, as keratinocytes move farther from the basement membrane, which is the link between the epidermal cells and their oxygen and nutrients' supplier (the dermal blood vessels), they receive fewer supplies, becoming less active and ultimately dying. Although this is a continuous development, 4 or 5 different *strata* with specific characteristics can be recognized in epidermis, varying the dimension of each *stratum* or even the number of *strata* with the body part from where the skin derives. From the deepest to the most superficial, those *strata* are the *stratum basale*, *stratum spinosum*, *stratum granulosum*, *stratum lucidum* and *stratum corneum* (Figure 1.2)<sup>9,11,12,14,17</sup>.

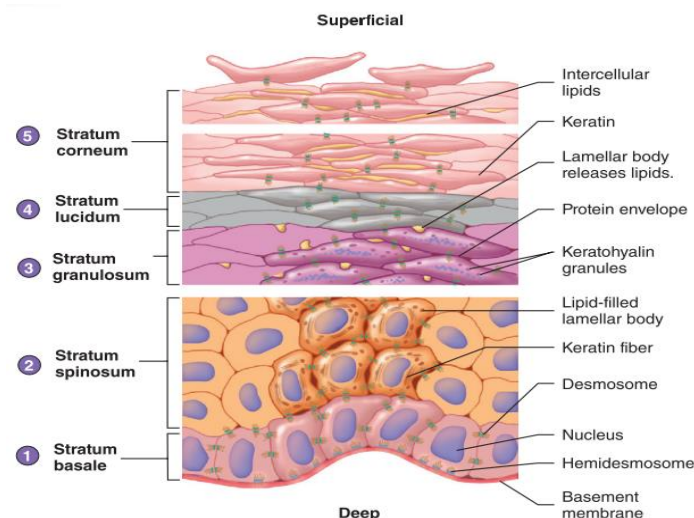


**Figure 1.2** - Epidermal differentiation: The different *strata* that compose epidermis and their main constituents. (Adapted from<sup>12</sup>)

***Stratum basale (SB)*** or ***Stratum germinativum*** is the innermost *stratum* of the epidermis and consists of a single layer of columnar cells, mitotically active, which generate new keratinocytes. From the mitotic division, one of the two daughter cells remains as a keratinocyte stem cell in the *stratum basale*, and divides itself during the next mitotic cycle, whereas the other daughter cell is shoved towards the surface and starts its differentiation process. The cells from this *stratum* have incorporated melanosomes, transferred by melanocytes, conferring some pigmentation and protection against UV light to this layer, and are adhered to each other by desmosomes and anchored to the basement membrane by hemidesmosomes, both contain keratin fibers that diffuse into the cell's cytoplasm. The keratins present in the cells from *stratum basale* are primary keratins with low molecular weight from type 5 and 14<sup>11,12,18</sup>.

***Stratum spinosum (SS)*** is the *stratum* directly above the germinativum cell layer and consists of a multiple layered *stratum* (8-10 cell layers) of many-sided cells. The name given to this *stratum* derives from an artifact produced during histological preparations, in which cells shrink increasing the intercellular spaces, except where they are linked by desmosomes, inducing a spiny appearance on cells. When arriving at this *stratum*, cells have already undergone a pressurizing process as they were pushed towards the surface, which led to their flattening and consequently to the break of the desmosomes previously formed, imposing the formation of new ones. In addition, envelope proteins and lamellar bodies (also known as keratinosomes), which are secretory organelles containing cholesterol, glycolipids and fatty acids as well as a battery of enzymes and antimicrobial peptides, are assembled in the cytoplasm. Later on, these membrane-coating granules will fuse with the plasma membrane of granular and *stratum corneum* cells and lipids will be released into the intercellular spaces, originating the extracellular matrix. The *stratum spinosum* presents not only K5/K14 keratins retained from the previous *stratum*, but also K1/K10 keratins, which are the keratins synthesized in this *stratum* and are accumulated as keratin fibers (tonofilaments). Therefore, the synthesis of type 1 and 10 keratins as well as lamellar bodies function as markers of the progressive differentiation<sup>11,12,19,20</sup>.

***Stratum granulosum (SG)*** is the middle *stratum* of the epidermis and consists of 2-5 layers of flattened, diamond-shaped cells that gradually start dying. The cells of this *stratum* exhibit a notorious specific feature, from which the *stratum's* name derived, which is the presence of dark keratohyalin granules in the cytoplasm. These granules contain numerous proteins, such as profilaggrin, loricrin and involucrin, crucial both for aggregation of keratin filaments and formation of the cornified envelope. During this stage, lamellar bodies formed in the previous *stratum* move towards the plasma membranes, merge with these structures, and release their content into the extracellular spaces. Simultaneously a protein envelope arises beneath the plasma membrane of cells. In the outermost layer of *stratum granulosum*, the cell organelles as well as the nucleus begin to degenerate, leading to cells' death, and tight junctions are established between adjacent cells, assisting in the epidermal structural barrier. This *stratum* marks the transition from the metabolically effective *strata* to the dead cells' *strata*<sup>11,12,14</sup>.

***Stratum lucidum (SL)*** is the *stratum* located between the *stratum granulosum* and *stratum corneum* and is absent in the skin of most of the human body, being found only in areas where the skin is thicker, such as the palms of the hands, the soles of the feet and the fingertips. This *stratum* consists of 3-5 layers of flattened dead keratinocytes containing large amounts of keratin fiber yet with no visible keratohyalin granules. The keratohyalin instead of being accumulated in granules, have dispersed around the keratin fibers, causing a transparent appearance on the cells of this *stratum*<sup>12,14</sup>.

**Stratum corneum (SC)** is the outermost *stratum* of the epidermis and the final stage of keratinocytes' differentiation process. The thickness of this *stratum* is very variable, ranging from a few layers where the skin is thin and does not suffer from abrasion, to more than fifty in areas where the skin is thick and subject to a lot of abrasion. The *stratum corneum* consists of dead cornified squamous cells, called corneocytes, embedded in a lipid-enriched extracellular matrix, originating a "brick and mortar" organizational model. The corneocytes, due to the previous degeneration of all organelles, only incorporate a protein envelope, comprised by loricrin, involucrin, trichohyalin and small proline-rich proteins crosslinked, as well as keratin fibers enclosed in filaggrin. As to the lipidic extracellular matrix, it results from the processing of the pro-barrier lipids by the lipolytic enzymes, both previously enclosed on the lamellar bodies, and incorporates 13 species of ceramides, cholesterol, and free fatty acids, as well as proteolytic enzymes and antimicrobial peptides. Corneocytes, because of their composition and their constituents' organization, confer strength and elasticity to this *stratum* along with hydration and UV protection, whereas the extracellular matrix provides antimicrobial protection as well as impermeability to water and water-soluble substances, avoiding transepidermal water loss and regulating selective transepidermal absorption. Additionally, *stratum corneum* presents an acidification of the environment relatively to the other *strata* of the epidermis, with pH values ranging between 4.5 and 5.5 instead of physiological pH values (7.35 - 7.45), derivative of endogenous mechanisms, which allows an effective enzymatic lipid processing for the assemble of the extracellular matrix, inhibits the early activity of the proteolytic enzymes and serves as a defense against pathogenic agents. The proteolytic enzymes have a crucial role in the upper layers of this *stratum* by degrading the corneodesmosomes, which are desmosomes that were modified during the terminal differentiation, allowing desquamation. According to the presence of corneodesmosomes and consequently the cellular cohesion, the *stratum corneum* can be divided in two sectors, which are *SC compactum*, in the deepest layers where cells are still strongly associated by corneodesmosomes, and *SC disjunctum*, in the most superficial layers where corneodesmosomes have already undergone proteolytic cleavage<sup>14,15,21-25</sup>.

Epidermis is a continually self-renewing epithelium as the desquamation rate of the cornified tissue and the proliferation rate in the basal layer are precisely balanced. As corneocytes slough off at the surface, new keratinocytes arise from the *stratum basale*, leading to a process of cellular ascension and transformation in chain, in which the cells below replace the cells directly above. A complete cycle of keratinocyte cytodifferentiation, since the cell is generated from the *stratum basale* until it reaches the epidermal surface and slough off takes approximately 40-56 days<sup>12,17</sup>.

### 1.1.2. PERMEATION ROUTES THROUGH SKIN

The skin is the interface between the organism and its external environment, consequently it is permanently in contact with several substances that are either present in the environment or intentionally applied to the surface of the tissue. Any substance, in order to enter the system and have any impact on the organism, positive or negative, must transpose the *stratum corneum* and reach viable cells. Even though *stratum corneum* is the primary barrier to skin penetration, the viable epidermis as well as part of the dermis also provide a significant permeability barrier to any substance that needs to enter the systemic circulation through the dermal capillary bed, penetrating through these layers<sup>8,26</sup>.

The permeation of a substance through skin might occur either via transepidermal pathway, in which molecules diffuse through the intact epidermis, or via transappendageal pathway, in which molecules diffuse through skin appendages, such as hair follicles and sweat glands. Additionally, when it occurs

via transepidermal pathway, particles can adopt either an intracellular route or an intercellular route. (Figure 1.3)

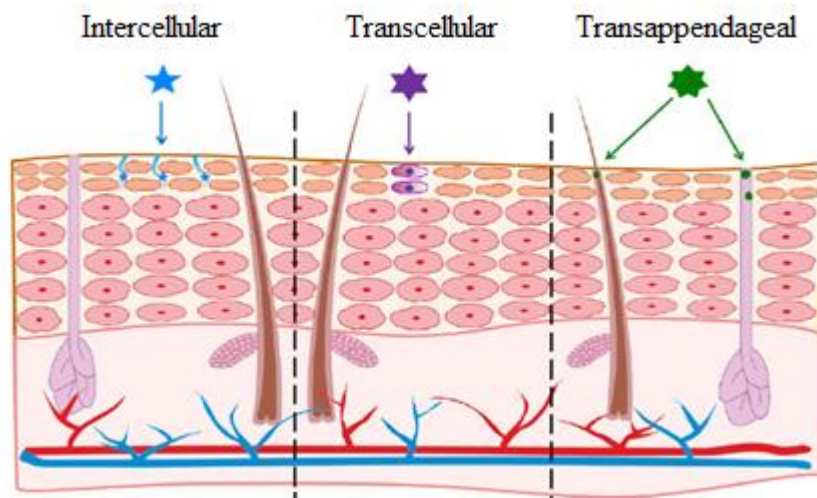


**Figure 1.3** - Pathways for permeation through the skin: Molecules diffuse either through the intercellular spaces, through keratinocytes or even through skin appendages. (Adapted from<sup>8</sup>)

The transappendageal pathway or ‘shunt’ route is considered to have a small contribution on the overall permeation process as skin appendages occupy only 0.1 % of the total skin surface, however, it is the only penetration pathway for particles larger than few nanometers. These appendages, due to their architectural structure, function not only as fast deliverers of compounds, that are capable of transfollicular penetration, to deeper skin layers and consequently into the systemic circulation, but also as reservoirs for substances which cannot overcome the transfollicular barrier<sup>8,27</sup>.

The transepidermal pathway is the main route for compounds penetration through skin, as it presents the major area available to the permeation process. The route through which compounds penetrate the *stratum corneum* and consequently the success of that penetration, differ according to the compound’s solubility and oil/water partitioning, usually described by the octanol-water partition coefficient ( $\log P$ )<sup>15,28</sup>.

By the **intracellular route**, also called transcellular route, the penetrating particles must diffuse through the alternating sheets of corneocytes and extracellular matrix. Even though the migration distance to overcome the epidermal barrier is shorter through this pathway, the consecutive alternation between hydrophilic (keratinocytes’ interior) and lipophilic (extracellular matrix) domains makes it a very selective route. Generally, the intracellular route is selected by the hydrophilic (polar) compounds, with low  $\log P$  values ( $\log P < 1$ ), which encounter greater energetic barriers while progressing through extracellular matrix due its lipidic nature<sup>8,28–31</sup>.

By the **intercellular route**, the penetrating particles, diffusing *stratum corneum* which are sized-restricted, progress through the extracellular matrix via passive diffusion, without intersecting any cells. When using this route, despite *stratum corneum* being a narrow layer, particles travel a much-extended pathway (sometimes 20 times longer than the thickness of the tissue), due to be a labyrinthine path. Generally, the intercellular route is preferred by the lipophilic (non-polar) compound, with intermediate/high  $\log P$  values ( $\log P > 3$ ), which have a high affinity to the lipidic composition of the matrix<sup>8,28,29,31</sup>.

The permeation process of any substance may occur either by a specific route or a combination of any of the possible routes. As different substances penetrate through human skin by different pathways, when assessing the barrier property of the skin, all different routes should be taken in consideration. Therefore, permeability studies integrate drugs with different polarities in order to evaluate the barrier function against a greater range of penetrability behaviors.

## 1.2. *IN VITRO* HUMAN SKIN MODELS

Skin models have been designed to attend both basic and applied research demands, therefore enabling skin cellular and molecular studies, for the better understanding of skin and its processes, as well as providing a foundation for the screening of new ingredients and active principles for safety and efficacy along with formulation optimization. Nowadays, skin models are also used for medical purposes as skin replacements or implants, however this use remains limited due to the lack of some components, such as vasculature, innervation and immunity system. Due to different demands, from either researchers or industries, different models have emerged revealing different levels of biological complexity<sup>2,10,32–36</sup>.

Monolayer cell cultures (2D models), which are cell cultures grown under contained flat conditions, have been the main approach for the study of both skin cell biology and pathophysiology *in vitro* as well as cellular responses to biophysical and biochemical stimulus. This method was the pioneer in the culture of human cells *in vitro*, with keratinocytes as the primary cell type, and since then has been widely used due to its simplicity, reproducibility and efficiency, allowing major advances in cellular knowledge<sup>37–39</sup>.

Although these models provide foundations for many scientific progresses, they are a reductionist approach that do not reproduce the complexity and dynamism of the *in vivo* tissues, producing frequently inconsistent results with those produced *in vivo*. Thus, 3D cell cultures were conceived in order to better mimic *in vivo* conditions, enabling the study of a wider range of biological processes<sup>38,39</sup>.

Skin tissue engineering (3D models), emerging as early as 1975 to 1980, produces fully differentiated tissues, which recreate architectural, metabolic, cellular and functional aspects of native human skin. These models comprise both cells and extracellular matrices and allow cells to grow and interact with their surroundings in all three dimensions, generating a natural gradient of nutrient access along with a waste buildup. Currently, the study of skin barrier function, wound healing, biological skin interactions, such as cell-cell and skin-microbiome interactions, as well as regulation of proliferation and differentiation of skin cells, relies on these models. The existing human skin models can be divided into three categories: (i) epidermal equivalents, which consist only of keratinocytes that differentiate producing a fully stratified epidermis; (ii) dermal equivalents, which consist of fibroblasts and collagen that interact generating a uniform contraction distinctive of dermis; and (iii) full-thickness skin equivalents, which consist of both dermal and epidermal layers. All three categories have, nowadays, commercially available prototypes developed by various companies such as CellSystems, StrataTech, SkinEthic, MatTek, Advanced Tissue Sciences, Organogenesis and more. Even though the resemblance of these 3D models to *in vivo* skin suggests that this approach should be adopted whenever possible, disadvantages such as high manufacturing cost, low reproducibility due to high complexity and absence of a standard approach, as well as low-throughput screening, limit its use<sup>9,10,34,36,37</sup>.

Despite the major progresses in scientific models, the existing designs are still not capable to entirely mimic the skin's natural environment, and further studies are required to develop improved models. Therefore, to assemble more physiological skin models, for both medical and screening purpose, intentions are to incorporate further skin components such as vasculature, immunity system, innervation,



appendages, pigmentation and adipose tissue into the pre-existing *in vitro* skin models, generating models of complete skin homeostasis. Additionally, to overcome the low reproducibility from the simplest to the most complex 3D models, 3D bioprinting presents itself as a promising method of model fabrication. Skin-on-a-chip is an existing revolutionizing method which incorporates skin equivalents in a device with a confined microenvironment and a microfluidic perfusion system. This technique has an enormous potential due to allowing a more controlled as well as automated tissue culture comprising dynamic perfusion, besides enabling a future integration on a multi-organ-chip<sup>10,40,41</sup>.

### 1.2.1. HUMAN EPIDERMAL MODELS

Despite more complex models, such as full-thickness skin equivalents, generally resemble native skin more reliably than simpler 3D models, their laborious manufacturing along with their high maintenance cost, due to their complexity, makes their use less frequent, being mostly accounted for more accurate and conclusive studies. Therefore, simpler skin equivalents like *in vitro* human epidermis, even though mimicking less well some properties from *in vivo* skin, are still subject of great interest for screening purposes<sup>2,7,42</sup>.

In the year of 1975, James Rheinwald and Howard Green tried, for the first time, to reconstruct epidermis by culturing primary human keratinocytes on top of a feeder layer of lethally irradiated 3T3 fibroblasts in an immersed environment. This experiment resulted in a small sheet of squamous epithelium with only 2 or 3 keratinocyte layers. Even though this approach was a major scientific breakthrough demonstrating that keratinocytes were capable of breed and form stratified colonies, these first epidermal models didn't present a normal differentiation pattern, lacking membrane-coating granules as well as a functional cornified layer, and consequently were far from resembling the native epidermal tissue. The first well-organized and fully differentiated epidermal model, evidencing both the inborn components that were missing, was only described in 1983 by Michel Pruni  ras when human keratinocytes were seeded on top of a cell-free dermal substrate and were left at air-liquid interface for 2 weeks. The exposure of keratinocyte cultures to an air-liquid interface stimulated the synthesis of membrane-coating granules, which consequently led to the formation of the extracellular matrix and ultimately allowed the cornification of the cells, establishing the *stratum corneum*<sup>2,43,44</sup>.

Over the years, culture media industry has evolved and specific culture media for culturing isolated keratinocytes without requiring the use of fibroblast co-cultures or dermal substrates, were developed. Those media are chemically-defined culture media supplemented with pro-differentiation factors, such as keratinocyte growth factor (KGF), calcium and ascorbic acid, which play a similar role to the one produced by the factors released by the dermis. Thus, nowadays 3D keratinocyte cultures can be accomplished by plating keratinocytes both on (i) a collagen matrix with fibroblasts; (ii) a collagen matrix without fibroblasts or a de-epidermized dermis; or even on (iii) inert filters<sup>2,6,45</sup>.

Due to the high demand for epidermal *in vitro* models, as the years went by several designs were developed and submitted to the European Center for the Validation of Alternative Methods (ECVAM) for validation of their use and commercialization. The first validated models arose in the 1990s by EpiSkin and MatTek Corporation being commercialized as EpiSkin<sup>TM</sup> and EpiDerm<sup>TM</sup>, respectively. Since then, many others emerged, resulting on the large variety of *in vitro* 3D reconstructed human epidermal (RHE) commercial models that are available nowadays<sup>2,6</sup>.

Although presently there is an immensity of RHE commercial kits available, which are of great value to research due to their standardized reproducibility and easy accessibility, their high cost and inflexible culture parameters force researchers to develop protocols for the conceiving of in-house RHE models, enabling a more cheaper and custom-made research<sup>2,36,46,47</sup>.

Currently, some standardized protocols stand for the reconstruction of in-house epidermal equivalents, which follow similar crucial steps (Figure 1.4). Firstly, keratinocytes are isolated from their source and cultured in monolayer cultures in order to increase the number of cells. In a second step, keratinocytes are seeded on a supports' surface, which can either be a biological matrix or an inert filter, undergoing immersed conditions so that they expand and cover the all surface. Finally, once a keratinocyte monolayer is established, cells are exposed to air-liquid interface which allows them to differentiate and stratify, resulting ultimately on a fully differentiated epidermis after 11 to 14 days.

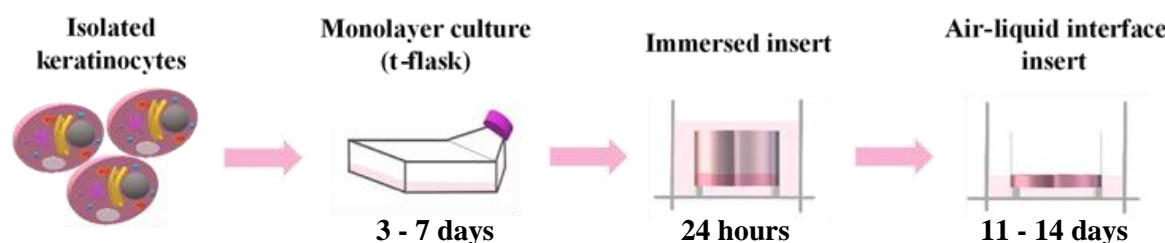


**Figure 1.4** - Crucial steps for the reconstruction of epidermal equivalents.

### 1.2.2. ATTEMPTS TO IMPROVE THE *IN VITRO* EPIDERMAL MODELS

The *in vitro* epidermal models produced so far, accurately resemble the morphological characteristics of the native human epidermis, however they do not entirely mimic the barrier function of the *in vivo* epidermal tissue. The barrier function of the *in vitro* models is reduced when compared to native epidermis, exhibiting much higher permeabilities (sometimes 10 times higher). Thus, many research studies have been developed in this field, aiming to identify the parameters which influence the formation of the skin barrier during epidermal tissue culture, in order to recreate an epidermal model with similar barrier properties to those found in the native skin<sup>2,7,37,48</sup>.

Studies have revealed that the lack of a normal barrier function by the epidermal models is related to deviations in lipid composition and packaging from *in vivo* human epidermis. Even though all major classes of human skin lipids are present in the *in vitro* RHE models and their arrangement into lipid lamellae is identical to the arrangement in the native epidermal tissue, some differences in the lipid profile may be the responsible for the existing differences on their packaging. Among the lipid profile discrepancies are the absence of ceramide 7 along with the low abundance of ceramide 4, 5, 6 and glucosylceramides contrasting with their high abundance in the native epidermis, the increased levels of monounsaturated free fatty acids (FFAs) although the levels of total FFAs are lower than the ones observed *in vivo*, the low values of cholesterol esters and high abundance of both ceramide 2 and triglycerides. These disparities are reflected in the arrangement of the lipid lamellae, which are found in a larger number but less densely packed than in native epidermal tissue<sup>2,7,32,49,50</sup>.

To diminish or even extinguish these variations between *in vitro* models and *in vivo* human epidermis, several attempts of improving the methods of culture have been made so far. Regarding to ceramides 6 and 7 (C6 and C7), was discovered that the addition of vitamin C to the media facilitated the synthesis of both ceramides, since it stimulates the hydroxylation of sphingoids and long chain fatty acids which are the precursors of both C6 and C7. Additionally, was also discovered that the addition of essential fatty acids such as arachidonic, palmitic, oleic and linoleic free fatty acids promoted the assembly of lamellar bodies, ceramides and cholesterol esters, since fatty acids are part of their composition. Along with the previous discoveries which resulted in positive outcomes as to improving the lipid profile and consequently the barrier formation, other modifications to the culture methods were tested. Amid the ones that produced satisfactory effects are the lowering of the relative humidity (RH) to 50% - 75%

instead of the 100% RH in which cultures were being incubated as well as the lowering of the temperature to 33 °C instead of the 37 °C (in order to better resemble the environment in which native skin grows), and also the supplementation of the culture media with vitamin D<sup>48-55</sup>.

Despite all the efforts, still no human epidermal equivalent has been able to fully mimic the barrier function of the *in vivo* epidermal tissue. Therefore, the search for a tissue culture recipe which produces an epidermal equivalent similar to the native human epidermis, in terms of morphology and barrier properties, continues<sup>2,48</sup>.

### 1.3. NEW ATTEMPTS TO IMPROVE THE *IN VITRO* EPIDERMAL MODELS

Even though many attempts have already been made to achieve an epidermis with an optimized barrier function, a multitude of alternatives are yet to be tested. The factors to consider when making changes to culture conditions can either be of environmental or nutritional nature. Whenever the desired test factor is environmental, modifications are made to the equipment to be adopted, either by choosing a different culture material from the usual or just by changing equipments settings; while when the desired test factor is nutritional, changes are made to the cell culture media composition. To assess the impact of the new culture conditions, environmental or nutritional, on the morphology and barrier properties of the epidermal tissue, histology and permeability tests must be performed on the epidermis reconstructed under modified conditions.

#### 1.3.1. CONDITIONS INTENDED TO SCREEN

The choice of culture conditions to be screened which could possibly improve the barrier properties of the *in vitro* skin, resulted from conflicting bibliography or divergent *in vitro* tissue culture protocols, from data previously acquired by the laboratory group through metabolomic analyzes performed on the culture media collected over the reconstruction of epidermal tissue or even from biological hints.

The first variation on the culture conditions proposed to assess was regarding to the **availability of autocrine and homocrine factors** during the air-liquid interface exposure. Many of the cellular processes, such as cell proliferation, migration, differentiation and apoptosis, are regulated by cell signaling, which occurs mostly by diffusion. The soluble diffusible signals can either be endocrine, when travel through the circulatory system in order to reach cells from other tissues, or paracrine, when they don't enter the bloodstream and only diffuse in between adjacent cells. Since in keratinocyte cultures there is no vasculature, only paracrine signaling is relevant in this type of *in vitro* cultures. Among the paracrine signals, some stimulate the cell that generated them, which are called of autocrine, other stimulate cells from the same cell type as the one that produced them, which are named homotypic paracrine or homocrine, and the ones that stimulate cells from a different cell type from the one in which the signal was created are termed heterotypic paracrine or simply paracrine. As in this *in vitro* cell culture only keratinocytes occur, just homocrine and autocrine signaling are present. During reconstruction of epidermal tissue, the media that supplies cells is renovated every other day, meaning that all signaling factors released by cells are disposed within a few hours leaving little time for action. In order to evaluate if an extended cellular exposure to homocrine and autocrine signals allows a greater proliferation and better differentiation of epidermal tissue, it was suggested to leave the medium unrenewed longer periods, while considering that the properties of the medium should be close to optimal. Thus, a preliminary study should be conducted to assess the acceptable extension of the media renewal period, without it losing its properties or accumulating too many toxic secreted compounds, and then the epidermal tissue grown under that same conditions would be analysed<sup>56,57</sup>.



The second variation on the culture conditions intended to assess was regarding to the **nutrients' availability** during the air-liquid interface exposure. A long time ago, epidermal culture protocols began to emerge in which the use of serum in culture media was eradicated, since it was a source of variability due to its unclear composition and inconsistency from one lot to the other, as well as a probable source of contamination due to its animal derivation. However, this supplement contains several growth factors, cytokines, hormones, vitamins and proteins that stimulate cell growth and proliferation, some of which are still unidentified, and thus makes it difficult to formulate a serum-free medium which fully resembles the serum-containing medium. Until now, several experiments have evaluated both epidermises reconstructed with serum-containing media and serum-free media, nonetheless contradicting results become apparent between research studies. Therefore, it was suggested that the medium used for the reconstruction of human epidermis was supplemented with fetal bovine serum (FBS), in order to assess the epidermal tissue reconstructed with serum-containing medium<sup>33,58–60</sup>.

The third variation on the culture conditions proposed to assess was regarding to the **temperature** during the air-liquid interface exposure. Most of mammalian cells are grown at 37 °C, temperature in which their growth rate is most efficient as it is their host's body temperature and both their enzymatic and protein machinery are adapted to operate optimally under those conditions. Yet skin cells are directly exposed to external temperatures that exhibit large variations, which causes average temperature at the surface of the skin to be close to 32 °C. Even though it is well-known that the temperature at the surface of the skin is lower than on the rest of the body, most of the studies on keratinocyte cultures have been conducted at normal body temperature, 37 °C, and only a few studies have been performed at 32 °C. Thus, it was suggested to culture epidermis at  $32 \pm 1$  °C, which is referenced by oecd guidelines for the testing of chemicals as the normal skin temperature, to evaluate whether the shift in the temperature at which the tissue is reconstructed significantly influences its properties. Considering that at lower temperatures cell metabolism is substantially decreased, a preliminary study should be conducted to assess how long it takes the epidermis to reach the differentiation level equivalent to the one attained after 12 days at 37 °C, and then the culturing of epidermal tissue under those conditions for that time period would be carried out<sup>61–64</sup>.

The last variation on the culture conditions intended to assess was regarding to the **oxygen availability** during the air-liquid interface exposure. Oxygen (O<sub>2</sub>) is crucial for cells to generate a chemical potential that allows them to produce energy and consequently perform their vital functions. Fluctuations in its concentration can significantly influence various cellular processes such as cell growth, differentiation, signaling and free radical production. According to a metabolomic study performed by the laboratory group on the culture medium collected over the reconstruction of epidermal tissue, cells produced lactate and formate during culture, which was suggested to be an indicator of limited oxygen conditions. Thus, it was proposed that the oxygen availability was increased in order to evaluate whether an improvement was verified in the reconstructed epidermal tissue, which among other ways could be achieved by expanding the contact surface between the culture media and the incubator atmosphere. By increasing the area of contact, the oxygen diffusion zone would also increase and consequently the diffusion of oxygen through the medium to the cells would increment<sup>65–67</sup>.

### 1.3.2. FRANZ DIFFUSION CELLS

For the evaluation of skin permeation by measuring the amount of drug that passes across the skin, diffusion cells have become the industry standard methodology and consequently the most broadly used experimental equipment<sup>63,68</sup>.

The first diffusion cell was developed in 1970 by Thomas J. Franz, who design a simple experimental apparatus, the “Franz cell”, composed by a donor compartment, where the formulation was applied to a semipermeable membrane, and a receiver chamber, where samples could be withdrawn through a sampling port for drug release analysis. Over the years, various designs of diffusion cells have emerged in response to research needs, even though the fundamentals of the original template were always maintained. Nowadays, three main types of diffusion cells exist: Franz-type cell (vertical, one-chambered static diffusion cell), side-by-side cell (horizontal, two-chambered static diffusion cell) and flow-through cell (vertical, one-chambered non-static diffusion cell) (Figure 1.5)<sup>15,68,69</sup>.

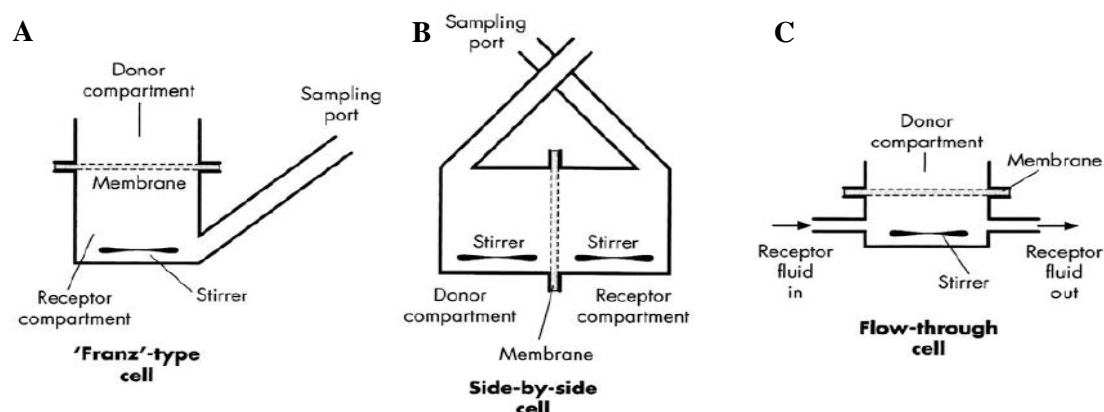


**Figure 1.5** - Three main types of diffusion cells: (A, C) Franz-type diffusion cell and Flow-through diffusion cell, respectively, both mainly used for *in vitro* percutaneous absorption studies; (B) Side-by side diffusion cell, mainly used for evaluation of skin immersed conditions. (Adapted from<sup>15</sup>)

Franz-type diffusion cells or upright static diffusion cells are the experimental apparatus used in the majority of *in vitro* percutaneous absorption studies, since it simulates the conditions most commonly encountered in the integumentary system of humans. In this device, the skin is hold between an upper opening to the ambient environment, as *in vivo* epidermis is exposed to the environment, and a lower compartment with a receiver solution. This layout allows the experiment of a wide range of formulations on skin surface, such as solutions, gels, creams, ointments, patches and other semi-solid materials of cosmetic or pharmaceutical nature. On the other hand, side-by-side diffusion cells or two-chamber diffusion cells are an experimental apparatus used in very limited situations, since it portrays circumstances in which *stratum corneum* is immersed in a liquid solution, such as while swimming or bathing, only allowing the experiment of compounds blended with that same liquid solution. In this device, the skin is hold between two horizontal compartments filled with aqueous solutions or other solvents, being one of them the donor solution where the permeant occurs and the other one the receiver solution. As to flow-through diffusion cells, they are an experimental apparatus used in the exact same circumstances as upright diffusion cells, since it follows the same basic principles of replicate the *in vivo* conditions. The difference between these two devices is that in the flow-through system the receptor fluid is continuously perfusing, mimicking the blood flow beneath the skin, which makes this device more suitable for full-thickness skin studies since in the integumentary system the bloodstream is never directly in contact with the epidermis. Due to this constant medium replacement, the solubilization of low solubility compounds is facilitated and sink conditions, which are an essential premise for the establishment of a proper *in vivo-in vitro* correlation, are maximized. Despite the advantages, the technical features associated with this mechanism represent not only a possible source of problems but also increase the commercial prize of the equipment<sup>15,68–70</sup>.

Currently, regulations as to *in vitro* skin absorption studies only partially standardize the experimental protocols as well as equipment design. Hence, researchers have a broad margin of flexibility to adapt

the experimental apparatus to the objectives of the experiment, since methodologies vary with aspects such as biological cells type, permeant nature, sampling intervals and dose levels. Regardless of the type of diffusion cell used, some features are imperative like the material from which cells are made be inert to the drugs tested (glass or Teflon are the most widely used), the temperature be maintained throughout the sampling period (either through a water jacket around each cell, an external water bath or warm air from a drying oven), the homogeneity within the receptor compartment be ensured (typically by employing a stirrer) and the sink conditions be guaranteed. Sink conditions ensure that the drug concentration in the receiver solution does not limit the permeation rate and are fulfilled when the drug concentration gradient between the donor compartment and the receptor compartment does not vary over 10% during the experiment<sup>9,15,68,69,71</sup>.

The recognition of Franz-type diffusion cells as a major research methodology to assess skin permeability resulted in a great demand for this experimental apparatus. Several companies currently manufacture Franz diffusion cells which exhibit the least variability within sets, however their excessive cost often motivates researchers to resort to less expensive alternatives such as hand-blown Franz cells in which variability rely upon the abilities of the technician<sup>71</sup>.

# CHAPTER 2

## MATERIALS AND METHODS

### 2.1. CELL CULTURING AND *IN VITRO* RECONSTRUCTION OF HUMAN EPIDERMIS

The *in vitro* reconstruction of human epidermis was performed using primary human epidermal keratinocytes (HEKn). This specific type of cells, isolated from neonatal foreskin, was purchased from Cascade Biologics (Portland, OR, USA), and kept cryopreserved until further use in liquid nitrogen as recommended by the producer.

When needed, the primary cells were thawed, inoculated and the cell culture maintained following the protocol provided by Cascade Biologics<sup>72</sup>. The consecutive procedures, such as trypsinization and reconstruction of human epidermis on polycarbonate filter, as well as the preparation of solutions, were performed according to the literature<sup>47</sup>.

All the procedures relative to the cell culture were performed in an aseptic environment using a vertical laminar flow chamber of biosafety class II type A/B3 (Nuair).

#### 2.1.1. PREPARATION OF SOLUTIONS

Prior to the beginning of the cellular culture, had to be ensured that all the solutions required along the procedures were available and prepared for use.

Although nearly all the solutions used in cell culture could have been prepared in the laboratory by the dissolution of solid reagents and posterior sterilization, most of the solutions were purchased already prepared and sterile as a way to ensure the uniformity and sterility. However, solutions resulting from the treatment of a purchased reagent, such as dialysed fetal bovine serum (DFBS) or from the mixing of several sterile liquid reagents, including blocking solution and freezing solution, still needed to be prepared prior to the step in which they were used. In addition, the medium for growing keratinocytes after purchase still needed to be enriched with supplements also purchased.

Medium is one of the most important reagents in cell culture, since it's what maintains cells alive and allow them to grow. For the keratinocytes culture, the chosen medium was EpiLife® Calcium-Free (Cascade Biologics) and its supplementation was according to the growth stage of the cells. Whereas, during the proliferation phase of keratinocytes only one supplementation of the medium was used, during the differentiation phase two medium variations were applied. Keratinocytes in monolayer culture, were fed with EpiLife supplemented with 0.06 mM CaCl<sub>2</sub> (Cascade Biologics) and 1% of human keratinocyte growth supplement (HKGS) (Cascade Biologics). After cells dissociation and seeding on the insert polycarbonate membrane, cells were firstly fed on medium containing EpiLife supplemented with 1.5 mM CaCl<sub>2</sub> and 1% HKGS, and 24hours after seeding that same medium was re-supplemented with 50 µg/mL of vitamin C (Sigma-Aldrich) and 10 ng/mL of keratinocyte growth factor (KGF) (R&D

Systems), resulting in a medium with which cells were fed until the end of differentiation (RHE medium). The increase of calcium from 0.06 mM to 1.5m M as well as the addition of vitamin C and KGF to the medium are essential during the phase of epidermis reconstruction in polycarbonate filter, since these elements are crucial for the stratification and differentiation of the keratinocytes. In addition, all culture media were also supplemented with a mixture of antibiotics (50 U/mL of Penicillin G and 50 µg/mL of Streptomycin) (Sigma-Aldrich), to prevent contaminations throughout the cell culture.

Fetal bovine serum (FBS) is a necessary element in the preparation of both blocking and freezing solutions nonetheless it has calcium in its constitution which will interfere with the final concentration of this component in those solutions and consequently impact the keratinocyte proliferation. Therefore, before using FBS (Biowest) for the preparation of the above-mentioned solutions, this serum was dialyzed in order to remove the unwanted chemical element. For this procedure were used Visking Dialysis Tubing membranes (Medicell Membranes Ltd) with a molecular weight cut off of 12,000 Da, that were washed to remove the glycerin coating. When introduced the FBS into the washed dialysis tubings (20 mL in each), they were sealed and boiled into 2 L of phosphate-buffered saline (PBS: 0.20g KCl, 0.24g KH<sub>2</sub>PO<sub>4</sub>, 8.00g NaCl, 1.44g Na<sub>2</sub>HPO<sub>4</sub> in 1L of distilled H<sub>2</sub>O, pH 7.4) at 4 °C with stirring. Every 3 hours the PBS solution was changed, up to a period of 12 hours, after which the solution was passed through a 0.2 µm filter (Pall Corporation) to ensure the sterility of the dialyzed fetal bovine serum (DFBS), and then stored in aliquots at -20 °C.

Blocking solution, which is used for the purpose of inactivating trypsin, is a simple solution that needs to be prepared prior to trypsinization. For its preparation were only needed Epilife medium and dialyzed fetal bovine serum, that were mixed in a proportion of 2:100, resulting in a solution of Epilife medium containing 2% DFBS.

Freezing solution is the blend where keratinocytes are kept cryopreserved and so, it is necessary to prepare it before starting the cryopreservation procedure. This solution has in its composition not only DFBS and Epilife medium, to nourish the cells, but also dimethylsulfoxide (DMSO) (Sigma-Aldrich), that works as a cryoprotective agent by slowing the cooling rate and reducing the risk of ice crystal formation, which can damage cells. Therefore, to prepare this solution, a mixture of 60% culture growth medium, 20% DFBS and 20% DMSO was assembled.

### 2.1.2. MONOLAYER CELL CULTURING

To initiate the keratinocyte culture, cells were firstly recovered from cold storage in liquid N<sub>2</sub> and promptly thawed in a warm bath at 37 °C, in order to avoid damaging from ice crystals.

Subsequently, keratinocytes had to be expanded and subcultured to ensure that they recovered from thawing and returned to their optimal proliferation potential to be used in the epidermis reconstruction. Therefore, the cell suspension was carefully transferred to a falcon containing culture media in order to dilute it to a seeding concentration of  $2.2 \times 10^4$  cells/mL. When the seeding concentration was obtained, 15 mL of suspension were inoculated to 75 cm<sup>2</sup> T-flasks. Cultures were placed in a humidified cell culture incubator (Nuair) at 37 °C, 5% CO<sub>2</sub>/95% air and left without any disturbance for 24 hours, allowing keratinocytes to adhere to the surface of the culture flasks.

Approximately 24 hours after the culture had been established, culture medium was replaced by freshly supplemented medium, to avoid further cell exposure to the dimethyl sulfoxide (DMSO) present in the freezing solution. Thenceforth, the culture growth was monitored recurring to inverted microscopy (Nikon Eclipse TE-2000S) (Figure 2.1), and the medium colour checked every other day. When a change in the medium colour, from pink to orange, was observed, the medium was changed since that indicated a shortage of nutrients and additionally a change in pH value unfavorable for the cells.

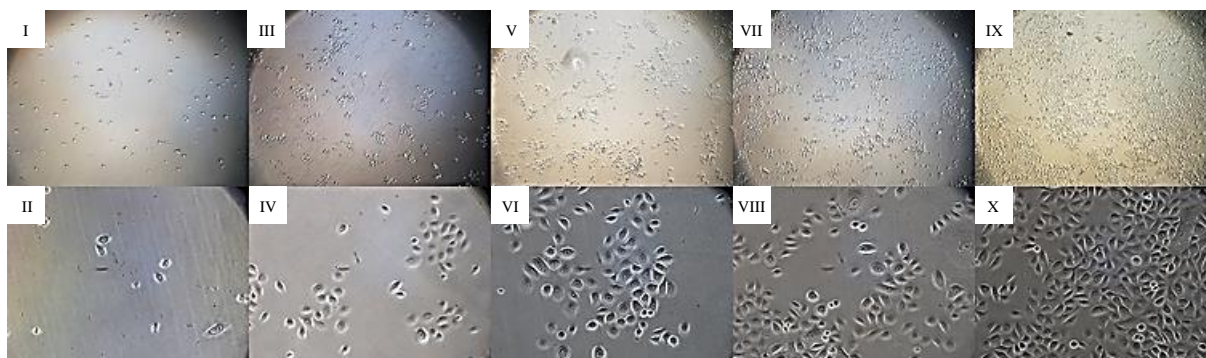


**Figure 2.1** - Monitorization of culture growth: Keratinocytes covering 10% (I, II); 20% (III, IV); 40% (V, VI); 60% (VII, VIII); 80% (IX, X) of t-flask surface. Magnifications: 40x (I, III, V, VII, IX); 200x (II, IV, VI, VIII, X)

Since cells at very high densities undergo growth inhibition and lose their proliferative potential, when keratinocytes reached a confluency of 70% - 80%, the detachment procedure was performed. Cultures were first washed with PBS, after which 3 mL of 0.05% trypsin-EDTA (Gibco) were applied, and flasks kept in the incubator for 7 minutes (or until cell detachment above 95% was observed on the inverted microscope). When most cells were dislodged, 12 mL of blocking solution were added to the suspension to block the action of trypsin on cells avoiding compromising their membranes. Subsequently the suspension was centrifuged for 7 minutes at 335 g and 4 °C in a Heraeus Sepatech Centrifuge Biofuge 28RS, in order to separate cells from the solution. The resulting supernatant was removed and the pellet, consisting of cells, resuspended in Epilife medium.

After trypsinization, cells could either be submitted to other subcultures (consecutive monolayer cultures), be cryopreserved or used to reconstruct a 3D tissue. Depending on the purpose thus the Epilife supplementation in which cells were resuspended and the final concentration to which they were.

In case the cells were to be cryopreserved, the pellet resulting from centrifugation was resuspended in non-supplemented Epilife medium in order to obtain a concentration of  $2 \times 10^6$  viable cells/mL and then the same volume of freezing solution was added to the suspension, thereby obtaining a final concentration of  $1 \times 10^6$  viable cells/mL for cryopreservation. Once the final concentration was achieved, keratinocytes were placed in a CoolCell® LX cell freezing container (Corning), which ensures a slow cooling essential for the cryopreservation of mammalian cells, and then placed in a -80 °C refrigerator for 24 hours. After 24 hours, vials could be finally moved to the gas phase of a liquid nitrogen tank (-178 °C) for storage.

### 2.1.3. RECONSTRUCTION OF HUMAN EPIDERMIS

As the objective of this work was to evaluate the effects of culture condition on the permeability of the resulting epidermis, the variations tested gave rise to multiple tissue culture protocols with only minor nuances between them. Therefore, the following protocol described was adopted as the standard and in table 2.1 were gathered the changes made to this same protocol for each test.

All cells used to reconstruct epidermis were from 4<sup>th</sup> passage, meaning that they had undergone 3 cycles of proliferation and trypsinization before being seeded in the polycarbonate filter to create the differentiated tissue.

When trypsinized keratinocyte purpose was to conceive the epidermal tissue, cells were resuspended in culture medium containing 1.5 mM  $\text{CaCl}_2$  to reach a cell density of  $3 \times 10^6$  viable cells/mL. Millicell® cell culture inserts with polycarbonate membrane, 12 mm of inner diameter and 0.4  $\mu\text{m}$  pore size (Merck Millipore) were placed in 6-well culture microplates using a sterile pair of tweezers and 2.5 mL of the



same medium used to resuspend keratinocytes were added to each well. Once the display needed to the reconstruction of epidermis was assembled, 500  $\mu\text{L}$  of cell suspension were added to the upper compartment of each insert and the plates were incubated in a humidified cell culture incubator at 37 °C, 5%  $\text{CO}_2$ /95% air. After 24 hours, time required to the adhesion of keratinocytes to the membrane, air-liquid interface was established on the cultures by aspiration of the culture medium within the insert and replacement of the medium from the well by 1.5 mL of medium for epidermis differentiation (RHE medium). Thenceforth, tissue cultures were maintained in the incubator for 11 days with the medium being renewed every other day.

After 11 days of air-liquid interface, fully differentiated epidermis were obtained.

Table 2.1 describes the test conditions selected in each experiment, as well as how the condition will vary comparatively to the standard (increasing or decreasing), if any preliminary testing is required to optimize the condition variation or to adjust the culture protocol to the condition under test, and finally summarizes the changes made to the standard culture protocol in order to evaluate each of the test conditions.

**Table 2.1** - Variations assessed in the culture conditions.

Condition varying	Increase/Decrease	Prior testing	Changes in the tissue culture protocol (after air-liquid interface establishment)
Availability of autocrine and homocrine factors	Increase	Epidermis were cultured either renewing media every 72 hours or every 96 hours.	Instead of renewing media every other day, media was renewed only every 72 hours.
Nutrients' availability	Increase	—————	Media used for epidermis differentiation (RHE medium) was additionally supplemented with 10% FBS.
Temperature	Decrease	Epidermis were cultured at 32 °C and samples were collected after 13, 18, 20, 22, 24, 27 and 30 days.	The incubator in which cells were incubated was at 32 °C instead of 37 °C, and the tissue culture was maintained for 21 days rather than 11 days.
Oxygen availability	Increase	—————	Cell culture inserts were placed in petri dishes with 85 mm of inner diameter instead of being placed in 6-well plates. The amount of media added to each well increased proportionally with the surface area (3.7 mL instead of 1.5mL).

## 2.2. ASSESSMENT OF EPIDERMIS' PERMEABILITY

After the required days to obtain a fully differentiated tissue, the barrier function of epidermis was assessed recurring to diffusion experiments<sup>36,73</sup>.

All diffusion studies were performed as described in the previously mentioned literature, employing hand-blown Franz-type diffusion cells (ITQB NOVA) (Figure 2.2 A) and using 3 transdermal model drugs with different polarities: caffeine (Alfa Aesar), a highly polar compound ( $\log P$  : -0.08)<sup>74</sup>; hydrocortisone (Alfa Aesar), a semi-polar compound ( $\log P$  : 1.43)<sup>74</sup>; testosterone (Sigma-Aldrich), a non-polar compound ( $\log P$  : 3.48)<sup>74</sup>. Since the available experimental apparatus (Figure 2.2 B) didn't allow to perform the 3 diffusion studies simultaneously, comprising 5 replicates each, the experiments were distributed for 3 consecutive days, being each model drug tested in a different day (caffeine, hydrocortisone and testosterone on the 11<sup>th</sup>, 12<sup>th</sup> and 13<sup>th</sup> day of tissue culture, respectively).



**Figure 2.2** - Diffusion studies equipment: Hand-blown Franz-type diffusion cell (A) and the complete experimental apparatus (B), in which 5 diffusion cells are dipped in a thermostatic bath maintained at a constant temperature.

For the experiments, saturated suspensions of the model drugs were prepared to supply the donor chambers of the Franz cells, in order to ensure a maximum thermodynamic activity and sink conditions. Those solutions were formulated in propylene glycol (PG) (Sigma-Aldrich), by mixing 3 g of caffeine or 1.8 g of hydrocortisone or 1.5 g of testosterone, depending on the model drug to be tested, to 3 mL of PG.

To fill the receptor compartments of the Franz cells (dimensions described in Appendix A), operating as receiver solution, a simple isotonic phosphate buffer solution (PBS) (pH 7.2) was used for caffeine and hydrocortisone diffusion studies, whereas for testosterone diffusion studies, the PBS solution had to be supplemented with a solubilizer due to the low solubility of testosterone in aqueous solvents. Since there were several solubilizers described in the literature to overcome this problem, a solubilization protocol was designed to study the best surfactant, among those available in the laboratory, to maximize the testosterone solubility. As a result of this preliminary study, 1% of polyoxyethylene-20-cetyl ether (Brij®58) (Sigma-Aldrich) was added to the PBS solution for testosterone diffusion studies.

### 2.2.1. TESTOSTERONE SOLUBILITY

In literature were described several solubilizers used in *in vitro* permeation studies to enhance the solubility of lipophilic compounds, such as bovine serum albumin (BSA), polyoxyethylenesorbitan



monolaurate (Tween®20), polyoxyethylene-20-cetyl ether (Brij®58) and octylphenoxy polyethyleneoxy-ethanol (Igepal®)<sup>36,75–77</sup>.

Prior to any testing, some of those surfactants were put aside due to the overlapping of the light absorbance peak of the surfactant with the one of testosterone, as it was the case with BSA<sup>78</sup>, or because it would be necessary to acquire new products, when others that performed the same function were already available, as it was the case of Igepal®. Therefore, only 2 surfactants (Brij®58 and Tween®20) were tested regarding their capacity of solubilizing testosterone.

To evaluate the potential of those solubilizers 3 solutions of 44 mL each were prepared, the first consisting only of PBS, which worked as control, other of PBS with 1% of Brij®58 (Sigma-Aldrich) and other of PBS with 1% of Tween®20 (Sigma-Aldrich). After solutions preparation, 8 mg of testosterone were added to each blend and a magnet was placed in each recipient, after which all solutions were put on a magnetic stirrer in order to solubilize testosterone.

At predetermined time points over the same 24 hours sampling period as in diffusion studies (after 1, 3, 5, 7, 10.5, 21 and 24 hours of agitation), solutions were withdrawn from the magnetic stirrer, centrifuged for 30 minutes at 400 g in order to settle the undissolved testosterone, and samples were collected from the supernatant in order to measure the dissolved portion of testosterone on the solution, recurring to spectrophotometry. After measuring the samples, the volumes taken were re-added to the main solutions, so that the portion solute/solvent wouldn't change, and the solutions were reinstated on the magnetic stirrer until the next time point or the end of the experiment.

### 2.2.2. DIFFUSION STUDIES

For the maintenance of temperature throughout the diffusion studies, as fluctuation of it can affect diffusion rates, experiments were performed in a thermostatic bath that was constantly kept at a temperature of  $37 \pm 0.5^\circ\text{C}$ . To guarantee the homogeneity of the receiver solutions in the lower chambers of Franz diffusion cells, each Franz cell was equipped with a magnet, allowing a constant stirring.

To initiate the diffusion studies, the receptor compartments of Franz diffusion cells were filled with the appropriate receiver solution, according to the model drug to be tested, cell culture inserts (with diffusional areas of  $0.7854\text{ cm}^2$ ) were assembled on the Franz cells and then the set up was placed into the water bath reservoir, where epidermis were left for 1 hour in order to hydrate. After hydration period, 500  $\mu\text{L}$  of saturated suspension were added to each donor compartment and then all orifices of Franz cells were coated with Parafilm®, to avoid evaporation.

At predetermined time points over the 24 hours sampling, (every 60 minutes up to 6 hours and after 10, 12 and 24 hours of diffusion)<sup>36</sup>, samples of 1 mL were taken from the lateral arm of the receptor compartment of Franz cells and volume immediately restored, by adding that same volume of fresh receiver solution.

After the end of each experiment, all collected samples were frozen at  $-20^\circ\text{C}$  in order to prevent any evaporation and subsequent concentration of the samples. When requested, the samples were thawed for analysis.

### 2.2.3. SAMPLES ANALYSIS

All samples collected from the diffusion experiments were analysed recurring to spectrophotometry, performed in a NanoDrop™ 2000c spectrophotometer (Thermo Fisher Scientific). The equipment

worked as a conventional spectrophotometer analyzing the radiation absorption of the samples in the ultraviolet and visible (UV-Vis) regions of the light spectrum (190 – 840 nm)<sup>79</sup>.

Prior to sample scanning, the wavelengths of the maximum absorbance peaks of each compound were validated, and calibration curves were drawn in order to enable the determination of model drugs concentration in the samples. For the caffeine and hydrocortisone solutions, the blank used was PBS, whereas for testosterone the blank used was PBS with 1% of Brij<sup>®</sup>58.

The detection wavelengths gathered matched what was in the literature, corresponding to 272 nm for caffeine, 247 nm for hydrocortisone and 243 nm for testosterone<sup>80,81,82</sup>. Thus, the samples collected from each experiment were scanned in the detection wavelength associated with the compound tested.

#### 2.2.4. DATA ANALYSIS

The values of absorbance compiled from the spectrophotometer were introduced in a spreadsheet, where through several functions were obtained the values of cumulative corrected amount of compound crossed per unit of area of skin in 24 hours ( $Q_{24}$ ) and the values of maximum flux at steady state ( $J_{max}$ )<sup>36,83,84</sup>.

First, by the direct application of the absorbance values in the Lambert-Beer law (Equation 2.1), the concentrations of the model drugs in the samples were obtained.

$$(2.1) \quad A_{\lambda} = c \times l \times \varepsilon_{\lambda}$$

where  $A_{\lambda}$  corresponds to the absorbance of the sample at the wavelength  $\lambda$ ,  $c$  to the concentration of the compound in the sample,  $l$  to the pathlength of the light through the sample and  $\varepsilon_{\lambda}$  to the extinction coefficient of the compound for the wavelength  $\lambda$ .

Then, by multiplying the samples concentrations by the volume of the receptor compartment, the mass of model drugs would be attained. However, since every time a sample was taken from the receptor compartment a portion of the compound was removed from the receiver solution, an adjustment had to be made for that part to be accounted for. Therefore, the total mass of drug that had crossed epidermis at a certain time was attained accordingly to the equation 2.2:

$$(2.2) \quad \text{Mass}_{\text{total}} = V_s \left( \sum_{n=1}^n C_{n-1} \right) + C_n \times V_r$$

where  $C_n$  corresponds to the concentration of sample  $n$  and  $V_s$  and  $V_r$  correspond to the volume of the sample and volume of the receiver solution, respectively.

Subsequently, the cumulative corrected amount of drug permeated, which is the amount of model drug that had crossed per unit of area of epidermis at a certain time, was calculated recurring to the equation 2.3:

$$(2.3) \quad \text{Cumulative Corrected Amount (Q)} = \frac{\text{Mass}_{\text{total}}}{\text{Cross-sectional area of tissue}}$$

By plotting the cumulative corrected amounts of drug permeated through epidermis ( $\mu\text{g}/\text{cm}^2$ ) as a function of time (h), it was possible to obtain the flux values ( $\mu\text{g}/\text{cm}^2/\text{h}$ ). The maximum flux values ( $J_{max}$ ) at steady state were thus given by the maximum slope of the linear portion of the graph, calculated by linear regression using at least 5 points.

Finally, once all the permeability parameters from all the experiments were gathered, the results from each culture condition variation were compared with the results obtained from standard culture

conditions. The statistical analysis was performed recurring to Sigmastat 4.0<sup>85</sup>, and significant mean differences were analysed using multiple comparisons by unpaired t-tests. To grant statistical significance to the analysis a p-value < 0.05 was selected.

### **2.3. HISTOLOGICAL ANALYSIS OF RECONSTRUCTED EPIDERMIS**

After the required days of culture to obtain a fully differentiated tissue, the morphology of epidermis was assessed recurring to histological analysis<sup>47</sup>.

The tissue removal from the inserts was performed with the use of a scalpel, and the subsequent fixation and preservation of the tissue, using formalin solution 10%, neutral buffered (Sigma-Aldrich). The remaining histological process was performed by the Histopathology Unit (HU) of the Instituto Gulbenkian de Ciência (IGC). The processing protocol of the samples includes the dehydration of epidermis, the embedding of the tissue in paraffin and its sectioning and staining, using hematoxylin and eosin (H&E stain).

When completed the histological preparation process, the samples were recovered from IGC and their morphology was analysed recurring to microscopy. In the morphological analysis were considered parameters such as thickness of the epidermis, stratification and differentiation of cells as well as uniformity within and between samples.

# CHAPTER 3

## RESULTS AND DISCUSSION

### 3.1. TESTOSTERONE SOLUBILITY

Once testosterone is one of the model drugs used for assessing epidermal permeability and the most non-polar one, the addition of a surfactant to the standard receiver solution (PBS) was required for its diffusion experiments. In order to select which solubilizer to add, a solubility study was carried out to evaluate which non-ionic detergent - between polyoxyethylenesorbitan monolaurate (Tween®20) and polyoxyethylene-20-cetyl ether (Brij®58) - best fulfilled the purpose. After completion of the assay, it was possible to draw fast and reliable conclusions from observation of the solutions (Figure 3.1), where a decreasing amount of unsolubilized testosterone could be observed from the PBS to the PBS + Tween®20 solution and consecutively to the PBS + Brij®58 solution.

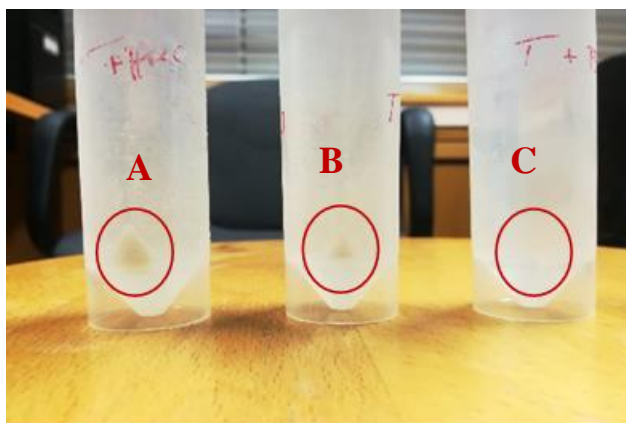


**Figure 3.1** - Unsolubilized testosterone, by visual inspection, in the different solutions after 24 hours of agitation: (A) PBS solution with a lot of testosterone non-solubilized, (B) PBS + 1% Tween®20 with some testosterone non-solubilized and (C) PBS + 1% Brij®58 with almost none testosterone non-solubilized.

Corroborating these prompt conclusions, were the results obtained by the analysis of the samples collected over the 24 hours of agitation, gathered in Figure 3.2. During the total stirring period, 1.74 g of testosterone were solubilized in pure PBS, while 5.32 g and 7.68 g of testosterone were solubilized in the PBS + 1% Tween®20 and PBS + 1% Brij®58 solutions, respectively. It was therefore concluded that both solubilizers had a positive effect on the solubilization of testosterone, which is in agreement with the literature<sup>36,76</sup>, nonetheless Brij®58 proved to be a better surfactant for testosterone dissolution in PBS. In response to these results, polyoxyethylene-20-cetyl ether was established as the testosterone solubilizer in the diffusion studies, with 1% being added to the PBS from the receptor compartment of Franz diffusion cell.

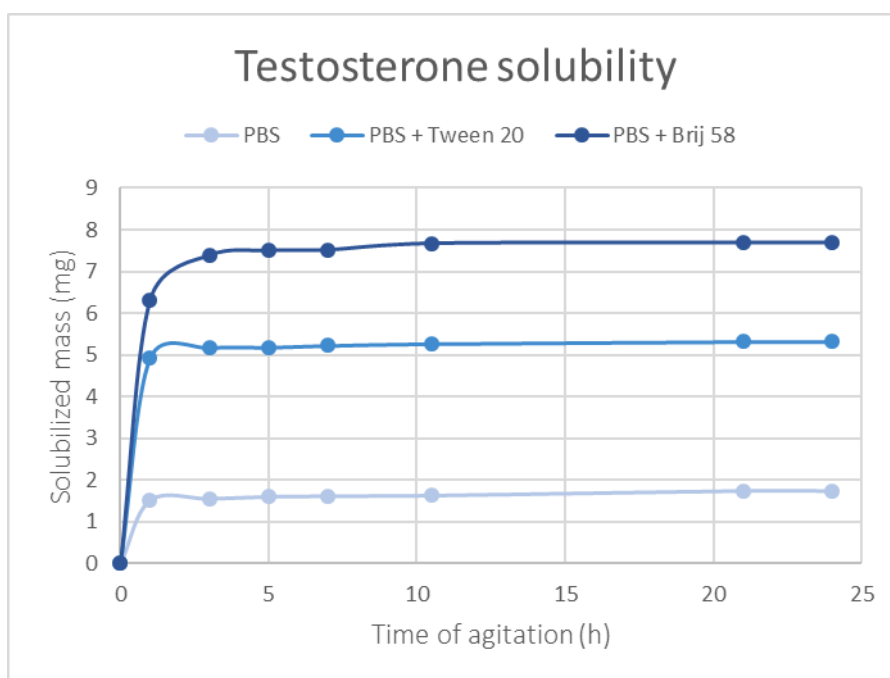


**Figure 3.2** - Testosterone solubility profile over 24 hours of agitation in the different solutions.

Although the intended objective of the study was achieved with the experimental protocol designed, it was found that the sampling period was not adjusted to the type of assay. During the first few hours major changes in testosterone solubilized mass occurred that weren't properly recorded, whereas from the 5<sup>th</sup> to the 24<sup>th</sup> hour of agitation many samples were collected and no significant changes in testosterone solubilized mass were observed. Then, in future solubility studies, it would be more accurate to have a higher sampling frequency over the first few hours and to reduce the total sampling period.

### 3.2. *IN VITRO* RECONSTRUCTION OF HUMAN EPIDERMIS AND ASSESSMENT OF ITS PERMEABILITY

Human epidermal keratinocytes were successfully cultured and expanded until 4<sup>th</sup> passage keratinocytes were obtained to reconstruct *in vitro* human epidermis.

To confirm the time of air-liquid interface required to obtain a fully differentiated epidermis with thickness equivalent to those described in the literature<sup>47</sup>, a tissue culture was performed in which one skin was collected on each day (10<sup>th</sup>, 11<sup>th</sup>, 12<sup>th</sup>, 13<sup>th</sup>, 14<sup>th</sup> and 15<sup>th</sup>). The culture times were selected regarding the standard air-liquid interface period described in literature (11<sup>th</sup>, 12<sup>th</sup> and 13<sup>th</sup> day), comprising the days surrounding this same period. After the collection of all samples, histological analysis was performed and both differentiation and thickness of epidermis were assessed. The results related to thickness are compiled in Figure 3.3 and expressed as average  $\pm$  standard deviation (SD). It shows that the thicker epidermis were from the 11<sup>th</sup>, 12<sup>th</sup> and 13<sup>th</sup> days of air-liquid interface, which exhibited  $49.28 \pm 2.11 \mu\text{m}$ ,  $54.01 \pm 2.11 \mu\text{m}$  and  $46.40 \pm 1.96 \mu\text{m}$  of thickness, respectively. Simultaneously, full differentiation was confirmed by visual recognition of epidermis main *strata* (*Stratum basale*, *Stratum Spinosum*, *Stratum Granulosum* and *Stratum Corneum*) in those samples, as it is shown in Figure 3.4. The results are in agreement with the ones described in the literature<sup>47,86,87</sup>, thus tissue cultures were maintained in the incubator at air-liquid interface for 11, 12 and 13 days, as stated in the standard protocol.

As the commercially available epidermal models for permeation studies, such as EpiDerm™ and Episkin®, have their thickness ranging from 30  $\mu\text{m}$  to 50  $\mu\text{m}$ <sup>32</sup>, the achieved thicknesses from the 11<sup>th</sup> to the 13<sup>th</sup> day were considered as good. However, when comparing to the thickness of native epidermal tissue, which ranges between 80-90  $\mu\text{m}$ <sup>32</sup>, the attained thicknesses were still deficient and so when seeking for a better model, the thickness is an element to have in consideration. The major difference observed in both in-house models and commercial models, comparing to native epidermis, is associated with the *stratum corneum*, which has neither the same lipid profile that interferes with packaging, as mentioned above<sup>7,32</sup>, nor the same thickness. The differences in thickness within the in-house epidermal models as well as between the in-house models and the commercial models are derived from various parameters that differ from protocol to protocol. Among those parameters is the time during which the culture is exposed to the air-liquid interface, the passage in which cells are used to form the epidermis, the medium used and the supplements added.

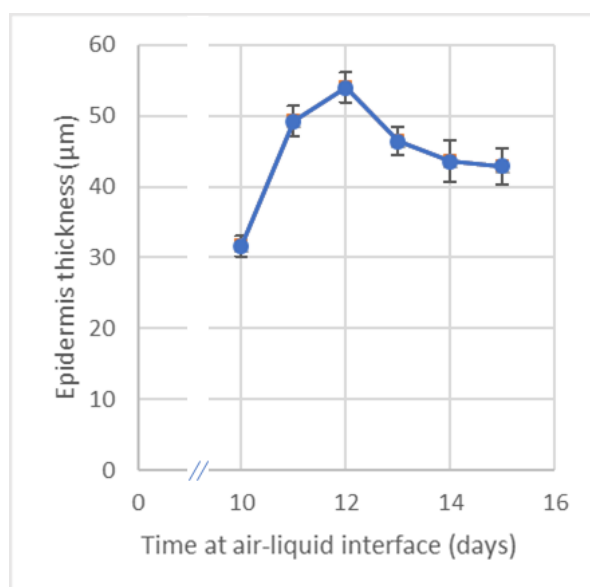


**Figure 3.3** - Evolution of epidermis thickness when cultivated at 37 °C, during the days surrounding the standard air-liquid interface period (n = 6, average  $\pm$  SD).



**Figure 3.4** - Fully differentiated epidermis with the *strata* that compose epidermis pointed out (approx. 54  $\mu\text{m}$  thick). Magnification 400x.



Epidermis were cultured according to the standard protocol and after 11, 12 and 13 days of air-liquid interface, tissues were collected for histological analysis and permeability tests.

By morphological analysis of the samples obtained from histology (Figure 3.5) it was confirmed the existence of a well individualized *stratum basale* along with a gradual cellular differentiation to *stratum spinosum* and then to *stratum granulosum*, all stained in shades of purple due to the presence of nucleus and other nucleic acids. As to *stratum corneum*, its existence was also confirmed by the pronounced pinkish coloration acquired by the tissue in its outermost layer, which is related to the large presence of proteins and lipids as well as lack of nuclei, distinctive features of this *stratum*. Thus, the epidermis obtained from this protocol were fully differentiated and stratified, plus exhibited an average thickness of 52  $\mu\text{m}$ , which matched the results obtained from the preliminary study.



**Figure 3.5** - Morphology of the reconstructed human epidermis grown under standard conditions, after 12 days at air-liquid interface (approx. 52  $\mu\text{m}$  thick). Magnification 400x.

By data analysis of the samples collected over the diffusion studies, parameters such as maximum flux ( $J_{\text{max}}$ ) as well as cumulative corrected amount of drug permeated through epidermis over the 24 hours ( $Q_{24}$ ) were obtained and subsequently compared to data from other skin models available in the literature. The results for the permeability parameters are gathered in table 3.1. In table 3.2 are compiled the data regarding other skin models available in literature. The values of both tables are expressed as average  $\pm$  SD. The permeability profiles for each model drug from which the parameters were determined are shown in Figures 3.6 to 3.8.

**Table 3.1** - Values obtained for the permeability parameters of the different model drugs in the reconstructed human epidermis (RHE) grown under standard conditions (average  $\pm$  SD).

Drugs	Permeability parameters	RHE (Standard conditions)
<b>Caffeine</b> (n=5)	$J_{\text{max}}$ ( $\mu\text{g}/\text{cm}^2/\text{h}$ )	$1411 \pm 109$
	$Q_{24}$ ( $\mu\text{g}/\text{cm}^2$ )	$50965 \pm 6270$
<b>Hydrocortisone</b> (n=4)	$J_{\text{max}}$ ( $\mu\text{g}/\text{cm}^2/\text{h}$ )	$8.013 \pm 2.074$
	$Q_{24}$ ( $\mu\text{g}/\text{cm}^2$ )	$178.5 \pm 27.2$

<b>Testosterone</b> (n=4)	Jmax ( $\mu\text{g}/\text{cm}^2/\text{h}$ )	$143.2 \pm 10.4$
	Q <sub>24</sub> ( $\mu\text{g}/\text{cm}^2$ )	$2595 \pm 112$

**Table 3.2** - Values obtained from bibliographic references for the permeability parameters of the different model drugs in commercial models and in human cadaver skin (average  $\pm$  SD).

Drugs	Permeability parameters	Literature			Human Cadaver (ref. <sup>36</sup> )
		Episkin® (ref. <sup>88</sup> )	EpiDerm™ (ref. <sup>36</sup> )	EpiDerm™ (ref. <sup>88</sup> )	
Caffeine	Jmax ( $\mu\text{g}/\text{cm}^2/\text{h}$ )	$10.59 \pm 2.81$	$11.0 \pm 1.7$	$2.12 \pm 1.77$	$0.7 \pm 0.1$
	Q <sub>24</sub> ( $\mu\text{g}/\text{cm}^2$ )	-	$210 \pm 79$	-	$11.0 \pm 0.9$
Hydrocortisone	Jmax ( $\mu\text{g}/\text{cm}^2/\text{h}$ )	-	$4.8 \pm 0.8$	-	$1.8 \pm 0.2$
	Q <sub>24</sub> ( $\mu\text{g}/\text{cm}^2$ )	-	$93.0 \pm 18.4$	-	$27.4 \pm 7.2$
Testosterone	Jmax ( $\mu\text{g}/\text{cm}^2/\text{h}$ )	$0.24 \pm 0.02$	-	$0.40 \pm 0.13$	-
	Q <sub>24</sub> ( $\mu\text{g}/\text{cm}^2$ )	-	-	-	-
Tamoxifen*	Jmax ( $\mu\text{g}/\text{cm}^2/\text{h}$ )	-	$6.3 \pm 2.4$	-	$2.8 \pm 0.8$
	Q <sub>24</sub> ( $\mu\text{g}/\text{cm}^2$ )	-	$69.4 \pm 5.2$	-	$91 \pm 30$

\*lipophilic compound (log P = 7.85) used in some studies.

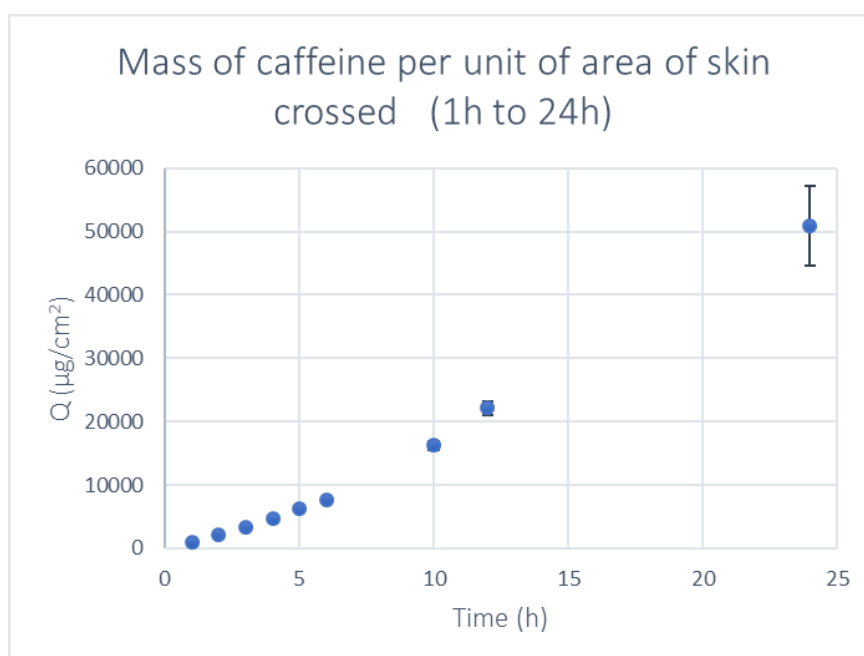


**Figure 3.6** - Caffeine permeability profile over 24 hours of sampling in reconstructed human epidermis (RHE) grown under standard conditions (n = 5, average  $\pm$  SD).



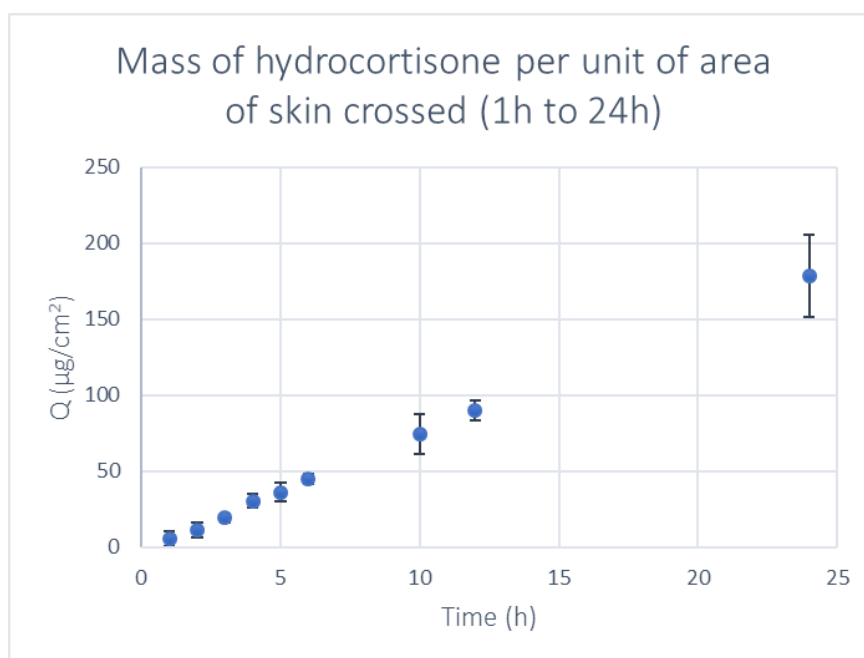


**Figure 3.7** - Hydrocortisone permeability profile over 24 hours of sampling in reconstructed human epidermis (RHE) grown under standard conditions ( $n = 4$ , average  $\pm$  SD).

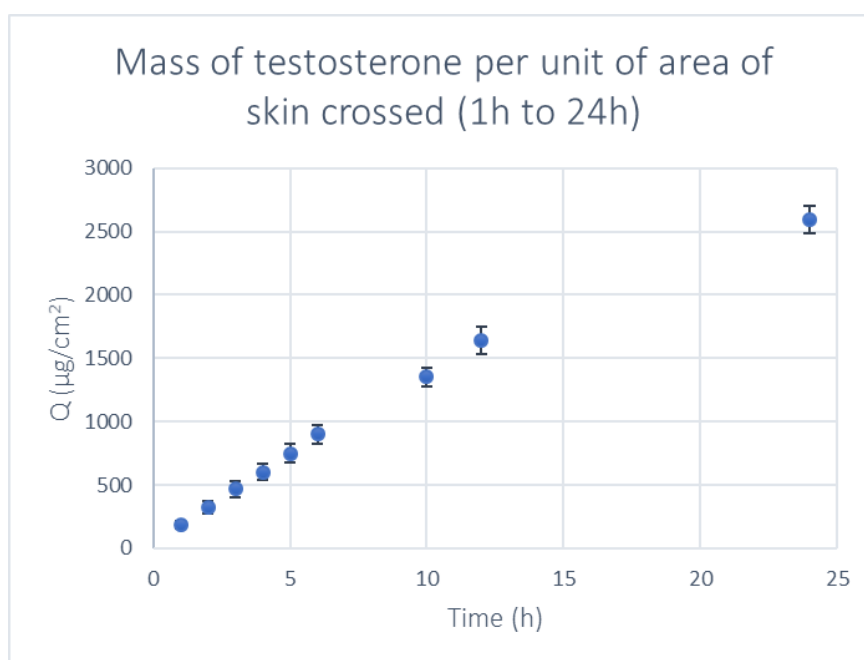


**Figure 3.8** - Testosterone permeability profile over 24 hours of sampling in reconstructed human epidermis (RHE) grown under standard conditions ( $n = 4$ , average  $\pm$  SD).

From the obtained results it was perceived that caffeine, the most polar of the tested compounds, was the one that presented the highest flow through skin ( $J_{max}$ ) as well as a greater amount permeated after 24 hours ( $Q_{24}$ ), followed by testosterone, the most non-polar compound, which presented permeability values of a much lower magnitude than caffeine yet still high, and finally by hydrocortisone, the semi-polar compound, which presented the lowest values of flux and drug amount permeated after 24 hours. When comparing the results obtained with those provided by the literature, it was verified that both reconstructed human epidermis and commercial epidermis models presented higher permeability values

for the most polar compound when compared to the other compounds studied, contrary to what is noted in native human skin, in which this compound is exactly the one that is least permeated by the tissue. These observations are in agreement with the previously mentioned, that the big difference observed between the existing models and the native skin is in the *stratum corneum*, since that layer is the primary responsible for preventing the passage of polar compounds due to the lipid matrix embedding the corneocytes. Additionally, it was perceived that both  $J_{\max}$  and  $Q_{24}$  values were considerably higher in reconstructed human epidermis than in commercial models. Despite this observation, it is not correct to directly compare these values as there are numerous divergences between the culture protocols and the conditions under which diffusion assays were performed.

### 3.3. ATTEMPTS TO IMPROVE THE BARRIER PROPERTIES OF *IN VITRO* EPIDERMIS

#### 3.3.1. AVAILABILITY OF AUTOCRINE AND HOMOCRINE FACTORS

The first attempt to improve the barrier properties of *in vitro* epidermis was by increasing the availability of autocrine and homocrine factors in the tissue culture medium. The method used to increase these resources' availability was by extending the intervals between medium renewals during epidermis culture, however the magnitude of the extension had to be previously studied. Therefore, a study was conducted in which 2 epidermis were grown in culture medium renewed every 72 hours and other 2 epidermis were grown in culture medium renewed only every 96 hours. As a result of this study, skins with an average thickness of 60  $\mu\text{m}$  were obtained from the cultures in which medium was renewed every 3 days (Figure 3.9 A), whereas skins with an average thickness of 41  $\mu\text{m}$  were obtained from the cultures where the medium was only renewed every 4 days (Figure 3.9 B). The disparity between average thicknesses was most likely due to the nutritional limitation that a medium renewal only every 4 days induces in the culture, thus limiting its growth. Hence, it was concluded that the optimal time to extend medium renewals was not 96 hours but 72 hours.

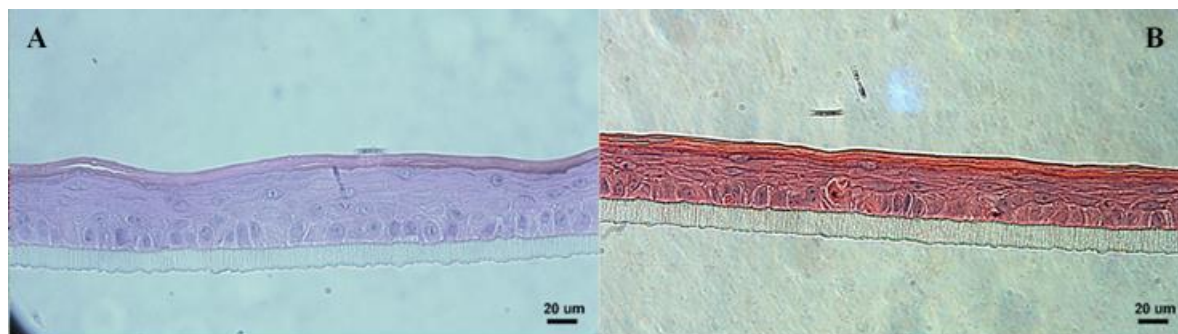


**Figure 3.9** - Morphology of (A) the reconstructed human epidermis grown in culture medium renewed every 72 hours (approx. 60  $\mu\text{m}$  thick) and (B) the reconstructed human epidermis grown in culture medium renewed every 96 hours (approx. 41  $\mu\text{m}$  thick), after 12 days at air-liquid interface. Magnification 400x.

Epidermis were cultured based on the standard protocol with the slight change that during air-liquid interface medium was renewed every 72 hours instead of every 48 hours. After 11, 12 and 13 days of air-liquid interface, tissues were collected for histological analysis and permeability tests.

Through morphological analysis of the samples attained from histology (Figure 3.10) it was promptly verified that the epidermis grown in culture medium renewed every 72 hours were, structurally, very similar to the epidermis grown under standard conditions, i.e. in medium renewed every 48 hours, exhibiting all the above mentioned *strata*, which allowed us to affirm that this adapted protocol also

generated totally differentiated and stratified tissues. Regarding to the epidermis thickness, an increase was detected when compared to epidermis grown under standard conditions, as epidermis grown in a less frequently renewed medium presented an average thickness of 65  $\mu\text{m}$ , which was in agreement with the results from the preliminary study. The difference in thickness was observed both in the living layer of the epidermis and in the *stratum corneum*, both presenting a greater thickness in the epidermis reconstructed according to the altered protocol.



**Figure 3.10** - Morphology of the reconstructed human epidermis grown in culture medium renewed only every 72 hours, after 12 days at air-liquid interface (approx. 65  $\mu\text{m}$  thick). Magnification 400x.

By data analysis of the samples collected over the diffusion studies, maximum flux ( $J_{\text{max}}$ ) as well as cumulative corrected amount of drug permeated through epidermis over the 24 hours ( $Q_{24}$ ) were determined and subsequently compared to those obtained from epidermis reconstructed in standard conditions. The results for the permeability parameters, expressed as average  $\pm$  SD, along with the statistical significance of their difference from the standard values are gathered in table 3.3. The permeability profiles for each model drug from which the parameters were determined are shown in Figures 3.11 to 3.13.

**Table 3.3** - Comparison of the values obtained for the permeability parameters of the different model drugs in the reconstructed human epidermis (RHE) grown in culture medium renewed only every 72 hours and in the reconstructed human epidermis (RHE) grown under standard conditions (average  $\pm$  SD).

Drugs	Permeability parameters	RHE (Standard conditions)	RHE (Testing conditions)	Statistical significance
<b>Caffeine</b> (n=5)	$J_{\text{max}}$ ( $\mu\text{g}/\text{cm}^2/\text{h}$ )	$1411 \pm 109$	$561.9 \pm 29.1$	p-value $\leq 0.001$
	$Q_{24}$ ( $\mu\text{g}/\text{cm}^2$ )	$50965 \pm 6270$	$23407 \pm 1107$	p-value $\leq 0.001$
<b>Hydrocortisone</b> (n=5)	$J_{\text{max}}$ ( $\mu\text{g}/\text{cm}^2/\text{h}$ )	$8.013 \pm 2.074$	$7.949 \pm 1.298$	p-value = 0.478
	$Q_{24}$ ( $\mu\text{g}/\text{cm}^2$ )	$178.5 \pm 27.2$	$181.8 \pm 26.5$	p-value = 0.430
<b>Testosterone</b> (n=5)	$J_{\text{max}}$ ( $\mu\text{g}/\text{cm}^2/\text{h}$ )	$143.2 \pm 10.4$	$34.86 \pm 2.16$	p-value $\leq 0.001$
	$Q_{24}$ ( $\mu\text{g}/\text{cm}^2$ )	$2595 \pm 112$	$962.6 \pm 169.6$	p-value $\leq 0.001$

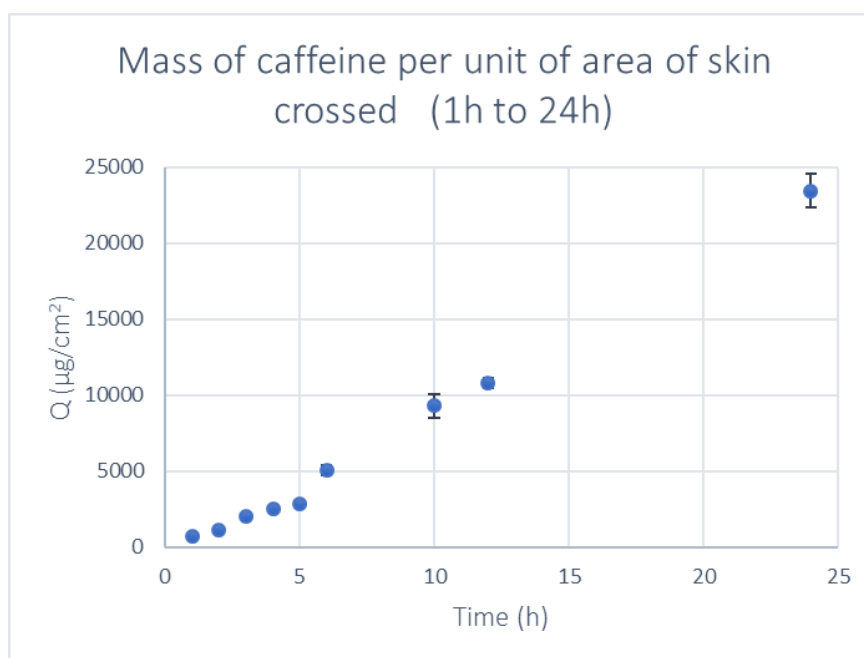


**Figure 3.11** - Caffeine permeability profile over 24 hours of sampling in reconstructed human epidermis (RHE) grown in culture medium renewed only every 72 hours. (n = 5, average  $\pm$  SD).

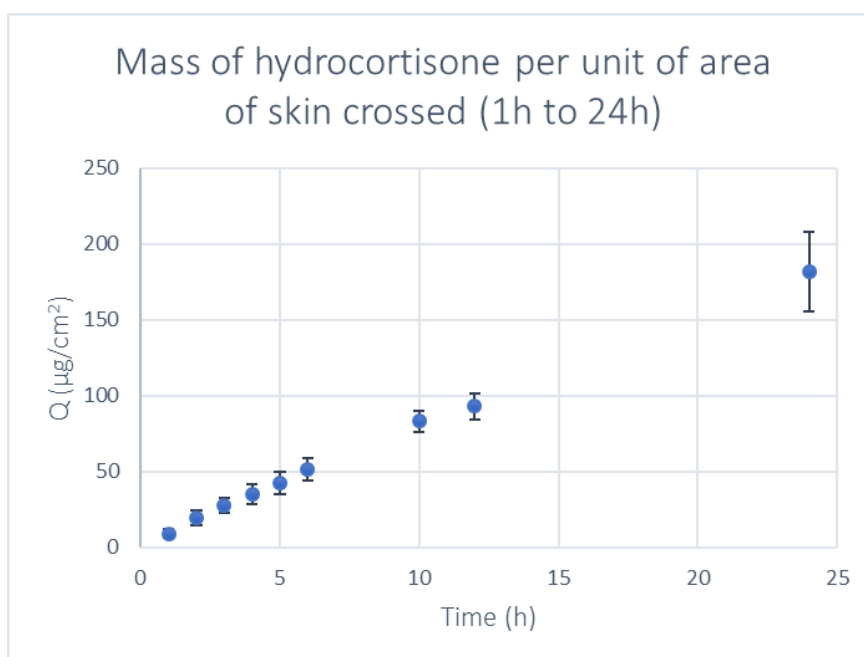


**Figure 3.12** - Hydrocortisone permeability profile over 24 hours of sampling in reconstructed human epidermis (RHE) grown in culture medium renewed only every 72 hours. (n = 5, average  $\pm$  SD).

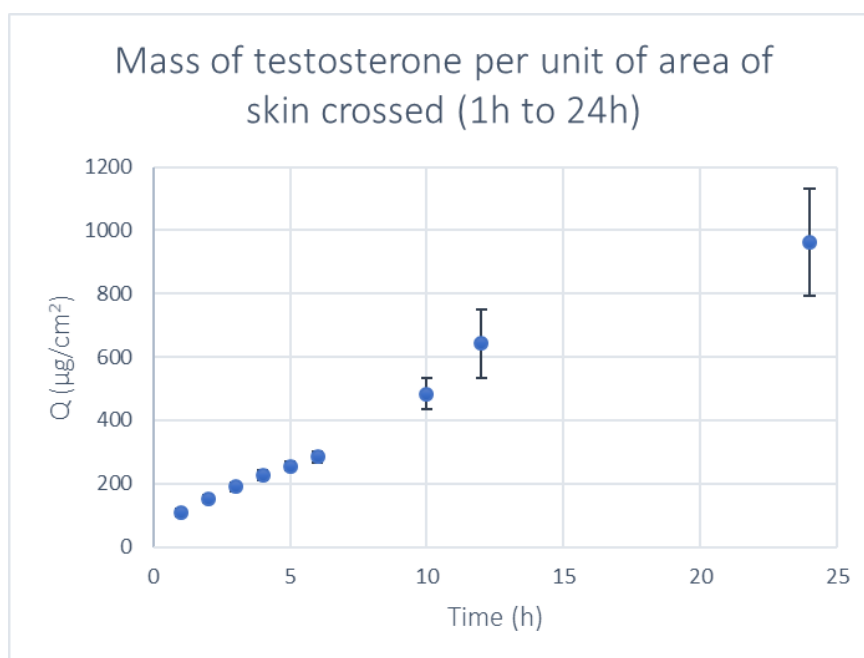


**Figure 3.13** - Testosterone permeability profile over 24 hours of sampling in reconstructed human epidermis (RHE) grown in culture medium renewed only every 72 hours. (n = 5, average  $\pm$  SD).

From the results obtained it was first noticed that caffeine remained the compound with the highest values of  $J_{max}$  and  $Q_{24}$ , as well as testosterone with the second highest values and hydrocortisone with the lowest values for both permeability parameters. When compared to the standard values, it was verified that both caffeine and testosterone decreased their  $J_{max}$  and  $Q_{24}$  values significantly ( $p \leq 0.001$ ), whereas hydrocortisone's  $J_{max}$  and  $Q_{24}$  values did not show statistically significant differences ( $p > 0.05$ ). The upgrade in epidermal tissue thickness perceived in the epidermis grown in culture medium renewed only every 72 hours was probably responsible for the improvement in caffeine and testosterone permeability, as the enlargement of the *stratum corneum* increased the caffeine permeation barrier and the enlargement of the living epidermis layer increased the testosterone permeation barrier. However, as hydrocortisone is a semi-polar compound and therefore has some affinity for both *stratum corneum* lipids and cells cytoplasm that comprise the living layer of epidermis, this upgrade was not significant to reveal differences in its permeation.

### 3.3.2. NUTRIENTS AVAILABILITY

The second attempt to improve the barrier properties of the *in vitro* reconstructed epidermis was by increasing the availability of nutrients in the tissue culture medium. The method used to increase these resources' availability was by supplementing the culture medium used in the epidermis reconstruction with 10% fetal bovine serum (FBS).

Epidermis were cultured based on the standard protocol with the slight change that the medium used to nourish cells during air-liquid interface was additionally supplemented with 10% FBS. After 11, 12 and 13 days of air-liquid interface, tissues were collected for histological analysis and permeability tests.

By morphological analysis of the samples obtained from histology (Figure 3.14) it was immediately revealed that the epidermis generated by this adapted protocol were poorly consistent and differentiated tissues. The tissues lacked a well-established *stratum basale* just as a well-shaped *stratum corneum*, which was perceptible by the discontinuous layer of cells attached to the polycarbonate filter and the tiny bright pink-colored outermost detached layer, respectively. In between them, a tangle of cells with

large gaps presented itself without much defined stratification. These findings sustained what was described on the literature<sup>89</sup> suggesting that the vitamin A included on the FBS had an inhibitory effect on the keratinocytes' differentiation, suppressing lipidic arrangements. An average epidermal thickness of 40  $\mu\text{m}$  was achieved however, little significance was given to these dimensions due to the deficient cohesion and the existence of gaps in the tissue.



**Figure 3.14** - Morphology of the reconstructed human epidermis grown in culture medium additionally supplemented with 10% FBS, after 12 days at air-liquid interface (approx. 40  $\mu\text{m}$  thick). Magnification 400x.

By data analysis of the samples collected over the diffusion studies, maximum flux ( $J_{\text{max}}$ ) as well as cumulative corrected amount of drug permeated through epidermis over the 24 hours ( $Q_{24}$ ) were determined and subsequently compared to those obtained from epidermis reconstructed in standard conditions. The results for the permeability parameters, expressed as average  $\pm$  SD, along with the statistical significance of their difference from the standard values are gathered in table 3.4. The permeability profiles for each model drug from which the parameters were determined are shown in Figures 3.15 to 3.17.

**Table 3.4** - Comparison of the values obtained for the permeability parameters of the different model drugs in the reconstructed human epidermis (RHE) grown in culture medium additionally supplemented with 10% FBS and in the reconstructed human epidermis (RHE) grown under standard conditions (average  $\pm$  SD).

Drugs	Permeability parameters	RHE (Standard conditions)	RHE (Testing conditions)	Statistical significance
<b>Caffeine</b> (n=5)	$J_{\text{max}}$ ( $\mu\text{g}/\text{cm}^2/\text{h}$ )	$1411 \pm 109$	$10916 \pm 476$	p-value $\leq 0.001$
	$Q_{24}$ ( $\mu\text{g}/\text{cm}^2$ )	$50965 \pm 6270$	$230472 \pm 25331$	p-value $\leq 0.001$
<b>Hydrocortisone</b> (n=5)	$J_{\text{max}}$ ( $\mu\text{g}/\text{cm}^2/\text{h}$ )	$8.013 \pm 2.074$	$89.65 \pm 2.78$	p-value $\leq 0.001$
	$Q_{24}$ ( $\mu\text{g}/\text{cm}^2$ )	$178.5 \pm 27.2$	$2080 \pm 111$	p-value $\leq 0.001$
<b>Testosterone</b> (n=5)	$J_{\text{max}}$ ( $\mu\text{g}/\text{cm}^2/\text{h}$ )	$143.2 \pm 10.4$	$141.2 \pm 16.3$	p-value = 0.421
	$Q_{24}$ ( $\mu\text{g}/\text{cm}^2$ )	$2595 \pm 112$	$2716 \pm 104$	p-value = 0.068



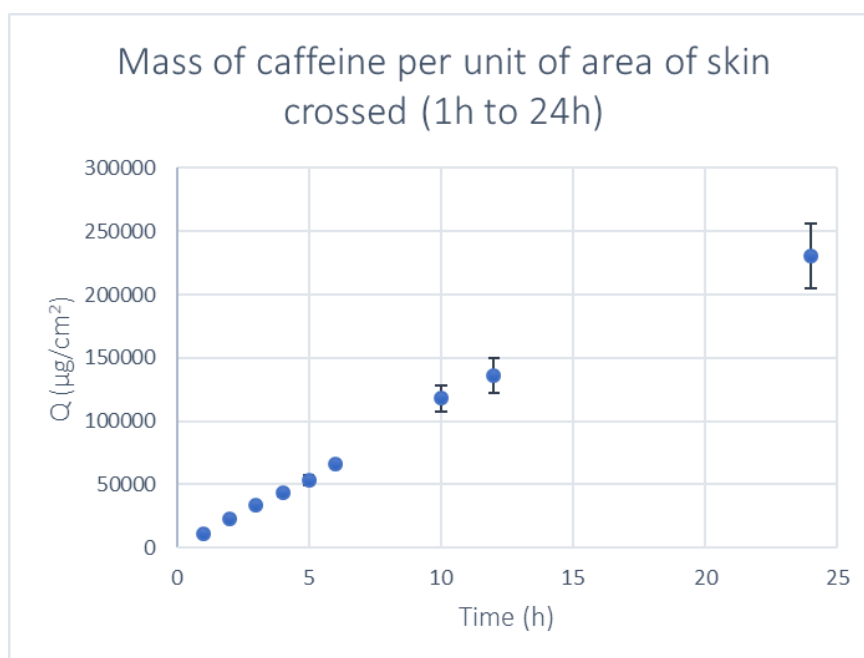


**Figure 3.15** - Caffeine permeability profile over 24 hours of sampling in reconstructed human epidermis (RHE) grown in culture medium additionally supplemented with 10% FBS. (n = 5, average  $\pm$  SD).

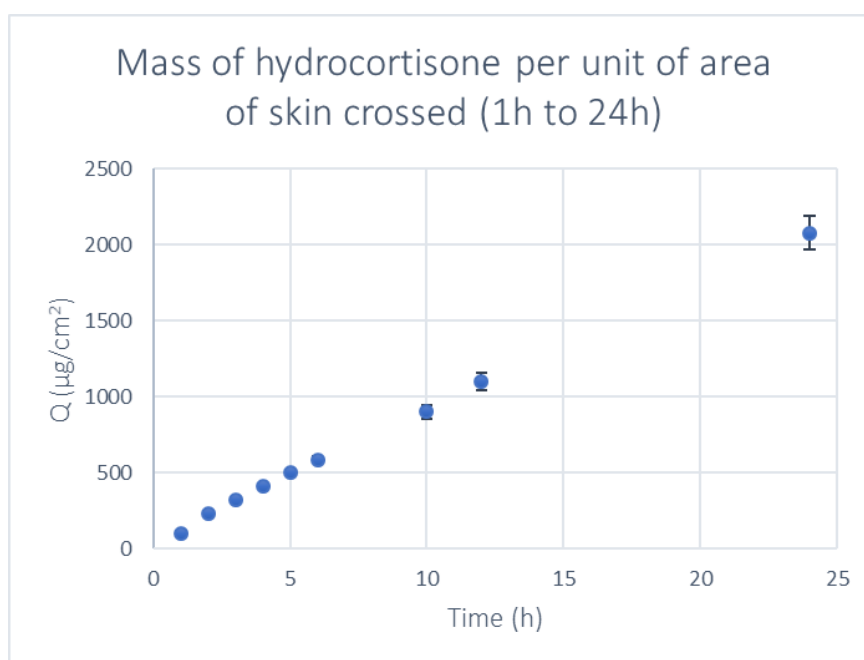


**Figure 3.16** - Hydrocortisone permeability profile over 24 hours of sampling in reconstructed human epidermis (RHE) grown in culture medium additionally supplemented with 10% FBS. (n = 5, average  $\pm$  SD).

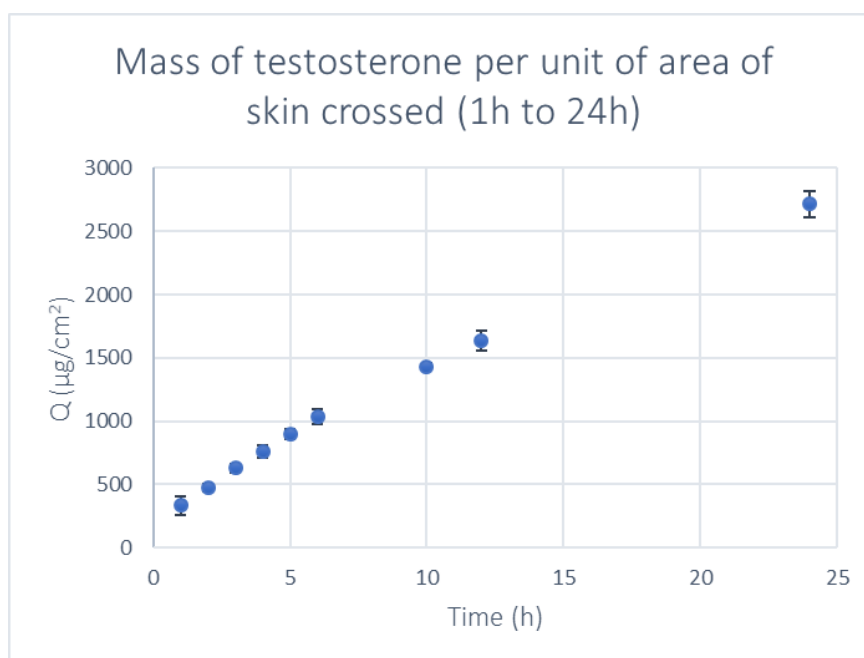


**Figure 3.17** - Testosterone permeability profile over 24 hours of sampling in reconstructed human epidermis (RHE) grown in culture medium additionally supplemented with 10% FBS. (n = 5, average  $\pm$  SD).

From the results obtained it was first noted that once again the order in which compounds were reported in terms of  $J_{max}$  and  $Q_{24}$  values repeated itself, yet with a clear proximity of hydrocortisone values to testosterone values for both permeability parameters. When compared to the standard values, it was verified that both caffeine and hydrocortisone increased their  $J_{max}$  and  $Q_{24}$  values significantly ( $p \leq 0.001$ ), whereas testosterone did not show statistically significant changes in its  $J_{max}$  and  $Q_{24}$  values ( $p > 0.05$ ). Probably the near absence of *stratum corneum* perceived in the epidermis grown in culture medium additionally supplemented with 10% fetal bovine serum was accountable for the worsening in caffeine permeability, since without that lipid-rich layer this polar compound did not encounter great barriers to its passage. This above-mentioned factor combined with the reduced tissue thickness and the presence of gaps in it may have also been responsible for the worsening of hydrocortisone permeability. Regarding testosterone, the lack of *stratum corneum* which would facilitate its passage through epidermis, counterbalanced with the existence of gaps in the living epidermal layer, which reduced its contact with the polar regions of epidermis, could be an explanation for the non-alteration of the permeability parameters values.

Possibly a reduction in the percentage of FBS added to the medium would be sufficient to reduce or even neutralize the negative effect of vitamin A and allow a positive effect of added nutrients to be noticeable.

### 3.3.3. TEMPERATURE

The third attempt to improve the barrier properties of the *in vitro* epidermis was by lowering the temperature to 32°C during tissue culture. Although this condition was achieved only by changing the incubator setting, it was known that a decrease in temperature would lead to a diminished cell metabolism and so it was necessary to extend the number of days at air-liquid interface required for epidermis to reach the same differentiation level as the one attained after 12 days of air-liquid interface at 37°C.



Therefore, a study was conducted in which several epidermis were grown at 32 °C and on predetermined days (13<sup>th</sup>, 18<sup>th</sup>, 20<sup>th</sup>, 22<sup>nd</sup>, 24<sup>th</sup>, 27<sup>th</sup> and 30<sup>th</sup>) two units were collected and both differentiation and thickness were assessed by histological analysis. The results related to thickness are compiled in Figure 3.18, proving that epidermis actually took longer to completely develop at 32 °C than at 37 °C, as describe in the literature<sup>61,64</sup>. Furthermore, it was determined that the best time lapse to obtain a fully grown and differentiated epidermis at 32 °C was after 22 days of air-liquid interface, when it was observed that the epidermis were fully differentiated and exhibited a thickness of  $68.55 \pm 5.44 \mu\text{m}$ . Hence, it was established that when cultures were maintained at 32 °C the air-liquid interface period was extended for 22 days and consequently the diffusion experiments were performed on the 21<sup>st</sup>, 22<sup>nd</sup> and 23<sup>rd</sup> day of air-liquid interface.

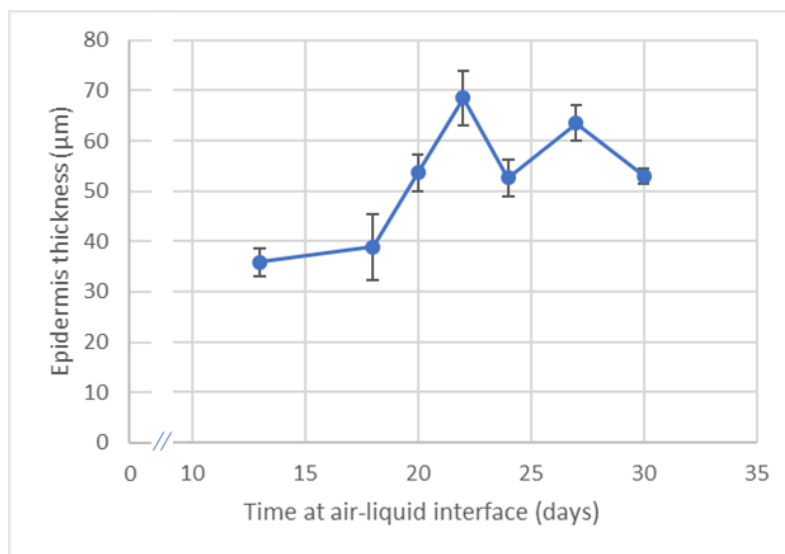


**Figure 3.18** - Evolution of epidermis thickness when cultivated at 32 °C, starting on the 13<sup>th</sup> day of standard air-liquid interface period and ending on the 30<sup>th</sup> day of air-liquid interface (n = 6, average  $\pm$  SD).

Epidermis were cultured based on the standard protocol with the slight change that the temperature in which cells were incubated during the air-liquid interface was 32 °C instead of 37 °C. After 21, 22 and 23 days of air-liquid interface, tissues were collected for histological analysis and permeability tests.

From morphological analysis of histology samples (Figure 3.19) it was revealed that epidermal tissue grown at 32 °C presented a complete differentiation and a high stratification. As in reconstructed epidermis grown under standard conditions, it was identified a well-defined *stratum basale* anchoring the tissue to the polycarbonate filter, a gradual cellular differentiation accompanied by the gradual flattening of cells that resulted in both *stratum spinosum* and *stratum granulosum* and finally an explicit enucleated *stratum corneum*. In the case of epidermis cultured at lower temperatures, an expanded *stratum corneum* was observed which inclusively displayed indicators of desquamation, a natural phenomenon that is responsible for the epidermal renewal by detachment of older corneocyte layers. The reconstructed epidermis derived from this adjusted protocol not only proved to be fully differentiated and stratified, but also exhibited an average thickness of 86  $\mu\text{m}$ , which indicated an improvement over epidermis reconstructed under standard conditions. The difference in average thickness obtained between the preliminary study and the conclusive study evidenced that sometimes there was some variability from batch to batch.



**Figure 3.19** - Morphology of the reconstructed human epidermis grown at 32 °C, after 22 days at air-liquid interface (approx. 86 μm thick). Magnification 400x.

By data analysis of the samples collected over the diffusion studies, maximum flux ( $J_{max}$ ) as well as cumulative corrected amount of drug permeated through epidermis over the 24 hours ( $Q_{24}$ ) were determined and subsequently compared to those obtained from epidermis reconstructed in standard conditions. The results for the permeability parameters, expressed as average  $\pm$  SD, along with the statistical significance of their difference from the standard values are gathered in table 3.5. The permeability profiles for each model drug from which the parameters were determined are shown in Figures 3.20 to 3.22.

**Table 3.5** - Comparison of the values obtained for the permeability parameters of the different model drugs in the reconstructed human epidermis (RHE) grown at 32 °C for 22 days and in the reconstructed human epidermis (RHE) grown under standard conditions (average  $\pm$  SD).

Drugs	Permeability parameters	RHE (Standard conditions)	RHE (Testing conditions)	Statistical significance
<b>Caffeine</b> (n=5)	$J_{max}$ ( $\mu\text{g}/\text{cm}^2/\text{h}$ )	$1411 \pm 109$	$440.8 \pm 29.1$	p-value $\leq 0.001$
	$Q_{24}$ ( $\mu\text{g}/\text{cm}^2$ )	$50965 \pm 6270$	$10294 \pm 2400$	p-value $\leq 0.001$
<b>Hydrocortisone</b> (n=4)	$J_{max}$ ( $\mu\text{g}/\text{cm}^2/\text{h}$ )	$8.013 \pm 2.074$	$9.153 \pm 0.960$	p-value = 0.178
	$Q_{24}$ ( $\mu\text{g}/\text{cm}^2$ )	$178.5 \pm 27.2$	$193.1 \pm 14.7$	p-value = 0.192
<b>Testosterone</b> (n=5)	$J_{max}$ ( $\mu\text{g}/\text{cm}^2/\text{h}$ )	$143.2 \pm 10.4$	$79.44 \pm 3.19$	p-value $\leq 0.001$
	$Q_{24}$ ( $\mu\text{g}/\text{cm}^2$ )	$2595 \pm 112$	$1530 \pm 37$	p-value $\leq 0.001$

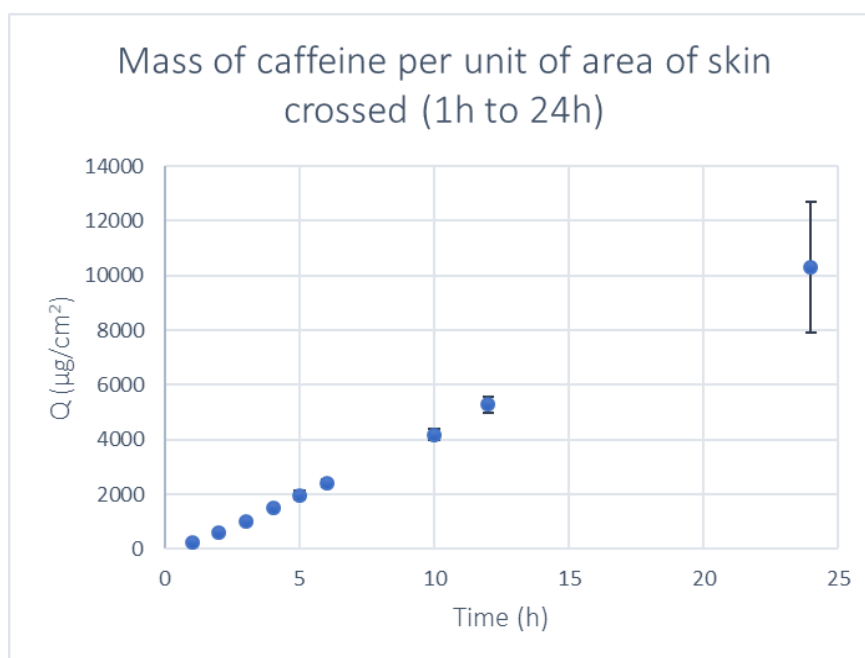


**Figure 3.20** - Caffeine permeability profile over 24 hours of sampling in reconstructed human epidermis (RHE) grown at 32 °C for 21 days. (n = 5, average  $\pm$  SD).

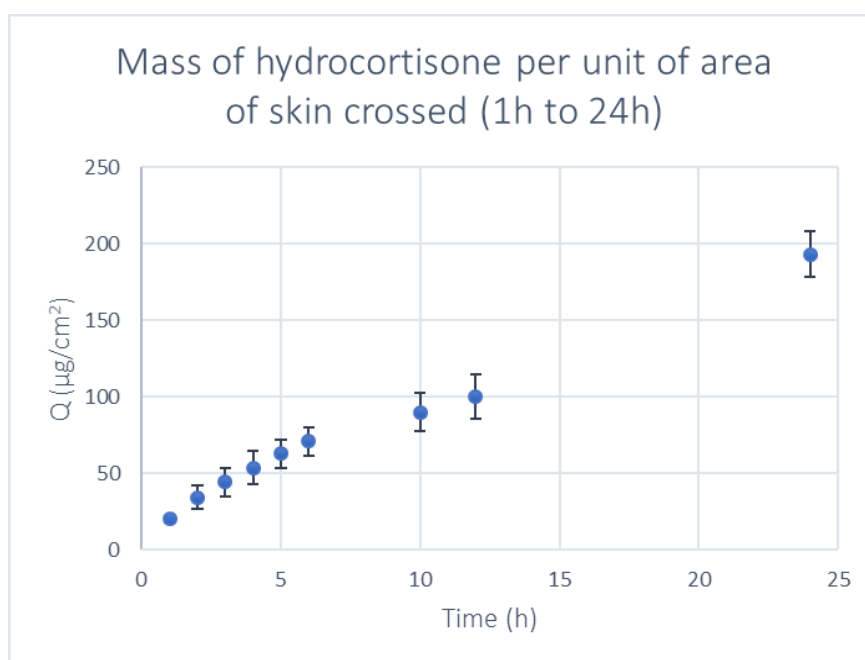


**Figure 3.21** - Hydrocortisone permeability profile over 24 hours of sampling in reconstructed human epidermis (RHE) grown at 32 °C for 22 days. (n = 4, average  $\pm$  SD).

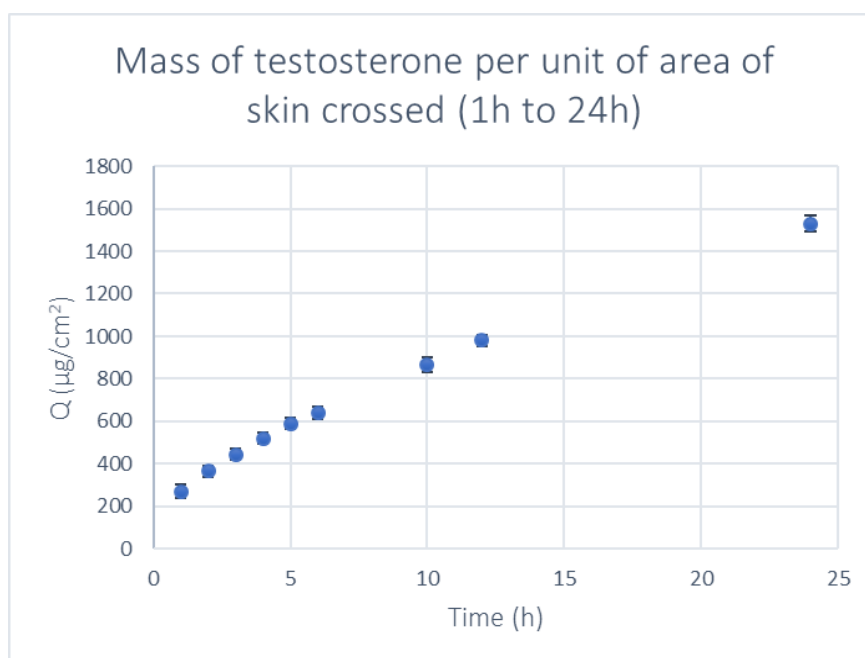


**Figure 3.22** - Testosterone permeability profile over 24 hours of sampling in reconstructed human epidermis (RHE) grown at 32 °C for 23 days. (n = 5, average  $\pm$  SD).

From the results obtained it was soon realized that caffeine remained the most permeated compound through the epidermis, exhibiting the highest values for both permeability parameters ( $J_{max}$  and  $Q_{24}$ ), and hydrocortisone the least permeated compound through the tissue. When compared to the standard values, it was verified that both caffeine and testosterone decreased their  $J_{max}$  and  $Q_{24}$  values significantly ( $p \leq 0.001$ ), whereas hydrocortisone did not show statistically significant differences in its  $J_{max}$  and  $Q_{24}$  values ( $p > 0.05$ ). These results were interpreted in the same way as those obtained when the availability of autocrine and homocrine factors was increased. As the overall thickness of the epidermis enhanced, both caffeine and testosterone experienced the enlargement of their permeation barriers, i.e. the *stratum corneum* and the living cell layer respectively, which led to the reduction of their permeability. The non-alteration of hydrocortisone permeability values in this morphological scenario was previously attributed to the affinity that this compound demonstrates to both layers, yet the marked increase in thickness verified in the epidermis cultured at 32 °C presupposed a decrease in its permeation. That was not the case and therefore, further studies would have to be conducted to understand the reason of this stagnation in the hydrocortisone's permeation.

### 3.3.4. OXYGEN AVAILABILITY

The last but not least attempt to improve the barrier properties of the *in vitro* epidermis was by increasing the availability of oxygen in the tissue culture medium. The method used to increase this resource's availability was by incrementing the contact surface between the culture medium and the atmosphere with petri dishes during the reconstruction of epidermis so that more oxygen was dissolved in the tissue culture medium and consequently more oxygen diffused into the cells.

Epidermis were cultured based on the standard protocol with the slight change that during air-liquid interface tissue culture inserts were in petri dishes instead of 6-well plates. After 11, 12 and 13 days of air-liquid interface, tissues were collected for histological analysis and permeability tests.

Through morphological analysis of the histologically examined samples (Figure 3.23) it was confirmed the establishment of a stratified and fully differentiated tissue in petri dishes, similar to the one obtained through the standard culture protocol in 6-well plates. All the *strata* that were noticeable in the standard epidermis were also recognized in the epidermis grown according to the redesigned culture protocol, however with a very slight increase in size of both *stratum corneum* and the living layer of epidermis. The average thickness accomplished was 56  $\mu\text{m}$ , which was close to that achieved under the standard conditions.



**Figure 3.23** - Morphology of the reconstructed human epidermis grown in petri dishes, after 12 days at air-liquid interface (approx. 56  $\mu\text{m}$  thick). Magnification 400x.

By data analysis of the samples collected over the diffusion studies, maximum flux ( $J_{\text{max}}$ ) as well as cumulative corrected amount of drug permeated through epidermis over the 24 hours ( $Q_{24}$ ) were determined and subsequently compared to those obtained from epidermis reconstructed in standard conditions. The results for the permeability parameters, expressed as average  $\pm$  SD, along with the statistical significance of their difference from the standard values are gathered in table 3.6. The permeability profiles for each model drug from which the parameters were determined are shown in Figures 3.24 to 3.26.

**Table 3.6** - Comparison of the values obtained for the permeability parameters of the different model drugs in the reconstructed human epidermis (RHE) grown in petri dishes and in the reconstructed human epidermis (RHE) grown under standard conditions (average  $\pm$  SD).

Drugs	Permeability parameters	RHE (Standard conditions)	RHE (Testing conditions)	Statistical significance
<b>Caffeine</b> (n=5)	$J_{\text{max}}$ ( $\mu\text{g}/\text{cm}^2/\text{h}$ )	$1411 \pm 109$	$1393 \pm 323$	p-value = 0.453
	$Q_{24}$ ( $\mu\text{g}/\text{cm}^2$ )	$50965 \pm 6270$	$49246 \pm 3407$	p-value = 0.302
<b>Hydrocortisone</b> (n=5)	$J_{\text{max}}$ ( $\mu\text{g}/\text{cm}^2/\text{h}$ )	$8.013 \pm 2.074$	$7.836 \pm 1.113$	p-value = 0.437
	$Q_{24}$ ( $\mu\text{g}/\text{cm}^2$ )	$178.5 \pm 27.2$	$187.3 \pm 18.2$	p-value = 0.290
<b>Testosterone</b> (n=5)	$J_{\text{max}}$ ( $\mu\text{g}/\text{cm}^2/\text{h}$ )	$143.2 \pm 10.4$	$100.5 \pm 6.3$	p-value $\leq 0.001$
	$Q_{24}$ ( $\mu\text{g}/\text{cm}^2$ )	$2595 \pm 112$	$2128 \pm 104$	p-value $\leq 0.001$

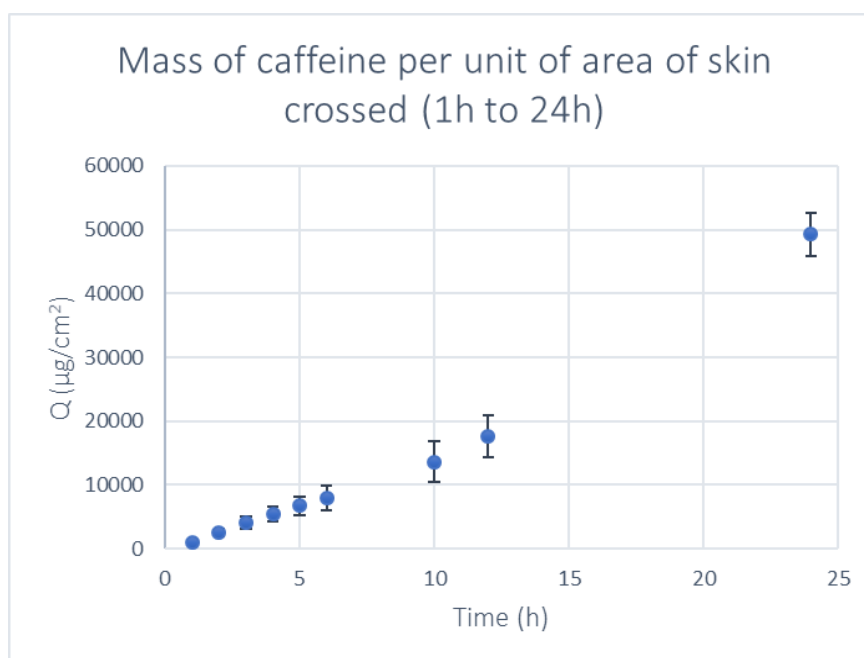


**Figure 3.24** - Caffeine permeability profile over 24 hours of sampling in reconstructed human epidermis (RHE) grown in petri dishes. (n = 5, average  $\pm$  SD).

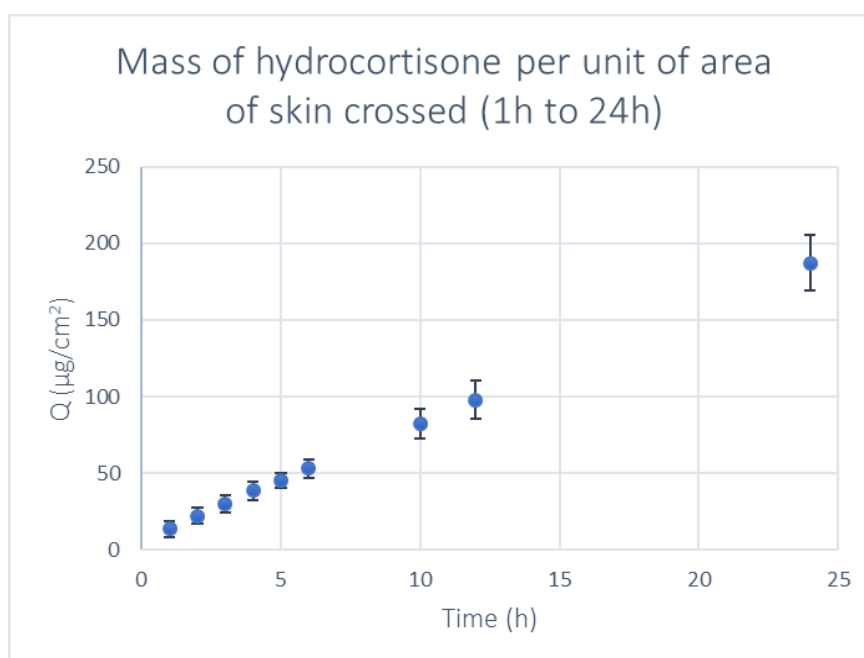


**Figure 3.25** - Hydrocortisone permeability profile over 24 hours of sampling in reconstructed human epidermis (RHE) grown in petri dishes. (n = 5, average  $\pm$  SD).

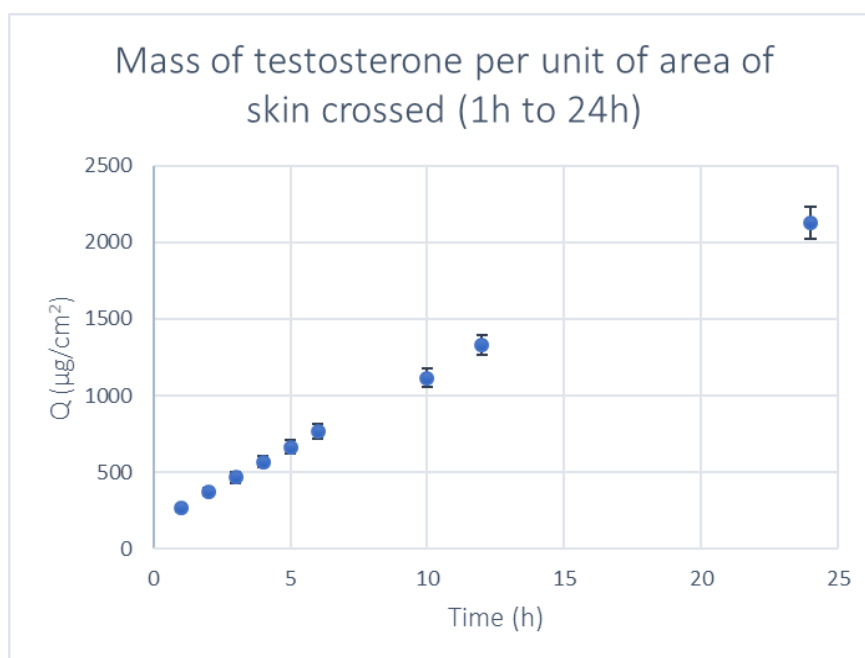


**Figure 3.26** - Testosterone permeability profile over 24 hours of sampling in reconstructed human epidermis (RHE) grown in petri dishes. (n = 5, average  $\pm$  SD).

From the results obtained it was first concluded that once again the polar compound was the one that most easily crossed the epidermis, presenting the highest values for  $J_{\max}$  and  $Q_{24}$ , the non-polar compound was the second most permeable and finally the semi-polar compound was the one that barely crossed the epidermis. When compared to the standard values, it was verified that both caffeine and hydrocortisone did not show statistically significant differences in their  $J_{\max}$  and  $Q_{24}$  values ( $p > 0.05$ ), whereas testosterone decreased its  $J_{\max}$  and  $Q_{24}$  values significantly ( $p \leq 0.001$ ). The permeability values of caffeine and hydrocortisone observed in these experiments remained similar, which is consistent with the morphological similarity shown between the tissues grown in 6-well plates and those grown in petri dishes. However, the improvement in testosterone permeability was not compatible with the conclusions drawn by direct morphological analysis. In order to find out why a decrease in testosterone permeability was observed, further studies would have to be conducted.

One possible study to better understand the behavior of this compound during the permeation assay would be by labelling the compound to allow the observation of its retention site and thus the cause of its slower progression through the epidermis. An alternative study would be to perform permeability tests on reconstructed epidermis grown both in 6-well plates and in petri dishes with non-polar compounds of different molecular dimensions in order to estimate whether intercellular spaces, through which these compounds penetrate, altered their size, either by cell size or cell confluency, and thereby restricted the passage of testosterone.



# CHAPTER 4

## CONCLUSION

The *in vitro* human epidermal equivalents that are currently cultured worldwide, with the purpose of providing a foundation for biotoxicity tests, drug screening as well as basic research, are still not adequate to fully mimic native human epidermis. The morphological characteristics presented by the *in vitro* models are similar to those presented by native skin, however the *in vitro* RHE barrier function is deficient when compared to the native epidermis, evidencing higher permeability values which require the extrapolation of results to clinical stages. Thus, the study of the parameters that can improve the properties of the cultured tissues is of great value for the development of more accurate models.

Any attempt on varying the tissue culture parameters to generate a model with a better barrier function is beneficial to the scientific community as it allows either to discard the attempted modification when it does not promote improvement in the model, or to recognize such modification as eventually advantageous when promoting enhancement.

Herein, various factors were assessed to understand their impact on the final *in vitro* model of RHE. The exposure to autocrine and homocrine factors, nutrient availability via FBS supplementation, temperature and oxygen availability were studied to understand their role in the formation of a good *in vitro* model, equivalent to human skin. The barrier function was enhanced through the modulation of the above-mentioned variables, except for the supplementation with FBS which resulted in poorly differentiated epidermis. On one hand, the increase in cellular growth factors, along with the decrease in incubation temperature resulted in an increase of epidermis thickness compared to the standard models and consequently in a reduced permeability to caffeine and testosterone, without altering the hydrocortisone permeability. On the other hand, the increase in oxygen availability has not shown to significantly affect epidermis thickness and therefore has not altered its permeability to both caffeine and hydrocortisone, however a reduction in testosterone permeability has been noticed. Variations in the permeability of the different compounds are found to be related not only with the thickness of the epidermal tissue, but also with the stratification and differentiation of each *stratum*, especially the *stratum corneum* in the final stage.

The results obtained along this study look promising although for more accurate and reliable results, repeatability and reproducibility assessments should be carried out. Also, in order to better understand the impact of changes in the standard protocol parameters on the cultured tissues, other tests complementary to histology and permeability tests, such as immunohistochemistry, lipid composition and organization evaluation or protein quantification should be considered. In an attempt to respond to the unanswered questions related to the impact of the conditions studied, the compounds retention on the skin could be assessed, the drug penetration profiles could be drawn, and/or other compounds with similar lipophilicity properties but different molecular properties could be tested.

Out of the four parameters herein tested, three of them (increased availability of cellular growth factors, lowered incubation temperature and increased availability of oxygen) have shown to improve the tissue



permeability characteristics, meaning that less compound has permeated through the tissue. This thesis provides a preliminary insight into how these parameters can affect the obtained RHE and how they can be adjusted to produce an *in vitro* model that better resembles the *in vivo* human epidermis, even though evidencing that there are many other parameters that need to be assessed to improve the understanding of their role in tissue development. Among the parameters that could improve this perception are the supplementation with proteins that are part of the protein envelope of the corneocytes, such as loricrin, involucrin, trichohyalin, small proline rich proteins, keratin and filaggrin, or the lipid supplementation with extracellular matrix lipids like ceramides, cholesterol and free fatty acids. A follow up of this work will eventually lead to the development of an optimized tissue culture protocol for the reconstruction of an *in vitro* epidermal model presenting a barrier function similar to the one found *in vivo*. The use of a more complex skin model, with keratinocytes being co-cultured with other types of cells, such melanocytes, Langerhans cells and Merkel cells or/and composed of both dermis and epidermis, would undoubtedly better mimic the native human epidermis and consequently generate results more feasible and with a closer relation to the *in vivo* ones.

# CHAPTER 5

## REFERENCES

1. Strategy&. *The Global Innovation 1000*. (2018). Available at: <https://www.strategyand.pwc.com/innovation1000>. (Accessed: 30th July 2019)
2. Pellevoisin, C., Bouez, C. & Cotovio, J. Cosmetic industry requirements regarding skin models for cosmetic testing. in *Skin Tissue Models* 3–37 (Academic Press, 2018). doi:10.1016/B978-0-12-810545-0.00001-2
3. Doke, S. K. & Dhawale, S. C. Alternatives to animal testing: A review. *Saudi Pharm. J.* **23**, 223–229 (2015). doi: 10.1016/j.jsps.2013.11.002
4. Ferdowsian, H. R. & Beck, N. Ethical and scientific considerations regarding animal testing and research. *PLoS One* **6**, e24059 (2011). doi: 10.1371/journal.pone.0024059
5. Liebsch, M. *et al.* Alternatives to animal testing: Current status and future perspectives. *Arch. Toxicol.* **85**, 841–858 (2011). doi: 10.1007/s00204-011-0718-x
6. Capallere, C. *et al.* Property characterization of reconstructed human epidermis equivalents, and performance as a skin irritation model. *Toxicol. Vitro.* **53**, 45–56 (2018). doi: 10.1016/j.tiv.2018.07.005
7. Mathes, S. H., Ruffner, H. & Graf-Hausner, U. The use of skin models in drug development. *Adv. Drug Deliv. Rev.* **69–70**, 81–102 (2014). doi: 10.1016/j.addr.2013.12.006
8. Dąbrowska, A. K. *et al.* The relationship between skin function, barrier properties, and body-dependent factors. *Ski. Res. Technol.* **24**, 165–174 (2018). doi: 10.1111/srt.12424
9. Sarmiento, B. *Concepts and models for drug permeability studies: Cell and tissue based in vitro culture models*. (Woodhead Publishing, 2015).
10. Abaci, H. E., Guo, Z., Doucet, Y., Jacków, J. & Christiano, A. Next generation human skin constructs as advanced tools for drug development. *Exp. Biol. Med.* **242**, 1657–1668 (2017). doi: 10.1177/1535370217712690
11. Pappas, A. *Lipids and Skin Health*. (Springer, 2015).
12. VanPutte, C. *et al.* *Seeley's Anatomy & Physiology*. (McGraw-Hill, 2014).
13. Hickman, C. P., Roberts, L. S. & Larson, A. *Integrated Principles of Zoology*. (McGraw Hill, 2001).
14. Tortora, G. J. & Derrickson, B. *Principles of anatomy & physiology*. (Wiley, 2014).
15. Moss, G. P., Gullick, D. R. & Wilkinson, S. C. *Predictive Methods in Percutaneous Absorption*. (Springer, 2015).
16. Breitskreutz, D., Mirancea, N. & Nischt, R. Basement membranes in skin: unique matrix

- structures with diverse functions? *Histochem. Cell Biol.* **132**, 1–10 (2009). doi: 10.1007/s00418-009-0586-0
17. Baroni, A. *et al.* Structure and function of the epidermis related to barrier properties. *Clin. Dermatol.* **30**, 257–262 (2012). doi: 10.1016/j.clindermatol.2011.08.007
  18. Shetty, S. & Gokul, S. Keratinization and its Disorders. *Oman Med. J.* **27**, 348–357 (2012). doi: 10.5001/omj.2012.90
  19. Elaine Fuchs. Epidermal Differentiation: The Bare Essentials. *J. Cell Biol.* **111**, 2807–2814 (1990). doi: 10.2307/1614286
  20. Raymond, A.-A. *et al.* Lamellar Bodies of Human Epidermis. *Mol. Cell. Proteomics* **7**, 2151–2175 (2008). doi: 10.1074/mcp.m700334-mcp200
  21. Menon, G. K., Cleary, G. W. & Lane, M. E. The structure and function of the stratum corneum. *Int. J. Pharm.* **435**, 3–9 (2012). doi: 10.1016/j.ijpharm.2012.06.005
  22. Haftek, M. *et al.* Compartmentalization of the human stratum corneum by persistent tight junction-like structures. *Exp. Dermatol.* **20**, 617–621 (2011). doi: 10.1111/j.1600-0625.2011.01315.x
  23. Candi, E., Schmidt, R. & Melino, G. The cornified envelope: A model of cell death in the skin. *Nat. Rev. Mol. Cell Biol.* **6**, 328–340 (2005). doi: 10.1038/nrm1619
  24. Elias, P. M. Stratum corneum defensive functions: An integrated view. *J. Invest. Dermatol.* **125**, 183–200 (2005). doi: 10.1111/j.0022-202X.2005.23668.x
  25. Chan, A. & Mauro, T. Acidification in the epidermis and the role of secretory phospholipases. *Dermatoendocrinol.* **3**, 84–90 (2011). doi: 10.4161/derm.3.2.15140
  26. Andrews, S. N., Jeong, E. & Prausnitz, M. R. Transdermal delivery of molecules is limited by full epidermis, not just stratum corneum. *Pharm. Res.* **30**, 1099–1109 (2013). doi: 10.1007/s11095-012-0946-7
  27. Patzelt, A. & Lademann, J. The increasing Importance of the Hair Follicle Route In Dermal and Transdermal Drug Delivery. in *Percutaneous Penetration Enhancers Chemical Methods in Penetration Enhancement: Drug Manipulation Strategies and Vehicle Effects* (eds. Dragicevic, N. & Maibach, H. I.) 43–53 (Springer, 2015). doi:10.1007/978-3-662-45013-0
  28. Harwansh, R. K., Patra, K. C. & Pareta, S. K. Nanoemulsion as potential vehicles for transdermal delivery of pure phytopharmaceuticals and poorly soluble drug. *Int. J. Drug Deliv.* **3**, 209–218 (2011).
  29. Ng, K. W. & Lau, W. M. Skin Deep: The basics of Human Skin Structure and Drug Penetration. in *Percutaneous Penetration Enhancers Chemical Methods in Penetration Enhancement: Drug Manipulation Strategies and Vehicle Effects* (eds. Dragicevic-Curic, N. & Maibach, H. I.) 3–11 (Springer, 2015). doi:10.1007/978-3-662-45013-0
  30. Trommer, H. & Neubert, R. H. H. Overcoming the stratum corneum: The modulation of skin penetration. A review. *Skin Pharmacol. Physiol.* **19**, 106–121 (2006). doi: 10.1159/000091978
  31. Van Gele, M., Geusens, B., Brochez, L., Speeckaert, R. & Lambert, J. Three-dimensional skin models as tools for transdermal drug delivery: challenges and limitations. *Expert Opin. Drug Deliv.* **8**, 705–720 (2011). doi: 10.1517/17425247.2011.568937
  32. Ponc, M., Boelsma, E., Gibbs, S. & Mommaas, M. Characterization of Reconstructed Skin Models. *Skin Pharmacol. Appl. Skin Physiol.* **15**, 4–17 (2002). doi: 10.1159/000066682
  33. Black, A. F. *et al.* Optimization and Characterization of an Engineered Human Skin Equivalent. *Tissue Eng.* **11**, 723–733 (2005). doi: 10.1089/ten.2005.11.723

34. Zhang, Z. & Michniak-Kohn, B. B. Tissue engineered human skin equivalents. *Pharmaceutics* **4**, 26–41 (2012). doi: 10.3390/pharmaceutics4010026
35. Groeber, F. *et al.* A First Vascularized Skin Equivalent as an Alternative to Animal Experimentation. *ALTEX* **33**, 415–422 (2016). doi: 10.14573/altex.1604041
36. Asbill, C. *et al.* Evaluation of a Human Bio-Engineered Skin Equivalent for Drug Permeation Studies. *Pharm. Res.* **17**, 1092–1097 (2000). doi: 10.1023/A:1026405712870
37. Niehues, H. *et al.* 3D skin models for 3R research: The potential of 3D reconstructed skin models to study skin barrier function. *Exp. Dermatol.* **27**, 501–511 (2018). doi: 10.1111/exd.13531
38. Duval, K. *et al.* Modeling Physiological Events in 2D vs. 3D Cell Culture. *Physiology* **32**, 266–277 (2017). doi: 10.1152/physiol.00036.2016
39. Teimouri, A., Yeung, P. & Agu, R. 2D vs. 3D Cell Culture Models for In Vitro Topical (Dermatological) Medication Testing. in *Cell Culture* 3–20 (IntechOpen, 2018). doi:10.5772/57353
40. Ng, W. L., Wang, S., Yeong, W. Y. & Naing, M. W. Skin Bioprinting: Impending Reality or Fantasy? *Trends Biotechnol.* **34**, 689–699 (2016). doi: 10.1016/j.tibtech.2016.04.006
41. Sriram, G. *et al.* Full-thickness human skin-on-chip with enhanced epidermal morphogenesis and barrier function. *Mater. Today* **21**, 326–340 (2018). doi: 10.1016/j.mattod.2017.11.002
42. Flaten, G. E. *et al.* In vitro skin models as a tool in optimization of drug formulation. *Eur. J. Pharm. Sci.* **75**, 10–24 (2015). doi: 10.1016/j.ejps.2015.02.018
43. Rheinwald, J. G. & Green, H. Serial Cultivation of Strains of Human Epidermal Keratinocytes: the Formation of Keratinizing Colonies from Single Cells. *Cell* **6**, 331–344 (1975). doi: 10.1016/S0092-8674(75)80001-8
44. Pruni  ras, M., R  gnier, M. & Woodley, D. Methods for Cultivation of Keratinocytes with an Air-Liquid Interface. *J. Invest. Dermatol.* **81**, 28s-33s (1983). doi: 10.1111/1523-1747.ep12540324
45. Seo, A., Kitagawa, N., Matsuura, T., Sato, H. & Inai, T. Formation of keratinocyte multilayers on filters under airlifted or submerged culture conditions in medium containing calcium, ascorbic acid, and keratinocyte growth factor. *Histochem. Cell Biol.* **146**, 585–597 (2016). doi: 10.1007/s00418-016-1472-1
46. Pedrosa, T. do N. *et al.* A new reconstructed human epidermis for in vitro skin irritation testing. *Toxicol. Vitro.* **42**, 31–37 (2017). doi: 10.1016/j.tiv.2017.03.010
47. De Vuyst, E. *et al.* Reconstruction of Normal and Pathological Human Epidermis on Polycarbonate Filter. *Epidermal Cells Methods and Protocols* 191–201 (2014). doi:10.1007/7651\_2013\_40
48. Sun, R. *et al.* Lowered Humidity Produces Human Epidermal Equivalents with Enhanced Barrier Properties. *Tissue Eng. Part C* **21**, 15–22 (2015). doi: 10.1089/ten.tec.2014.0065
49. Ponc  , M. *et al.* The Formation of Competent Barrier Lipids in Reconstructed Human Epidermis Requires the Presence of Vitamin C. *J. Invest. Dermatol.* **109**, 348–355 (1997). doi: 10.1111/1523-1747.ep12336024
50. Ponc  , M. *et al.* Lipid and ultrastructural characterization of reconstructed skin models. *Int. J. Pharm.* **203**, 211–225 (2000). doi: 10.1016/S0378-5173(00)00459-2
51. Fluhr, J. W. *et al.* Generation of Free Fatty Acids from Phospholipids Regulates Stratum Corneum Acidification and Integrity. *J. Invest. Dermatol.* **117**, 44–51 (2001). doi: 10.1046/j.0022-202x.2001.01399.x

52. Boyce, S. T. & Williams, M. L. Lipid supplemented medium induces lamellar bodies and precursors of barrier lipids in cultured analogues of human skin. *J. Invest. Dermatol.* **101**, 180–184 (1993). doi: 10.1111/1523-1747.ep12363678
53. Agren, J., Sjors, G. & Sedin, G. Ambient Humidity Influences the Rate of Skin Barrier Maturation in Extremely Preterm Infants. *J. Pediatr.* **148**, 613–617 (2006). doi: 10.1016/j.jpeds.2005.11.027
54. Ponc, M. *et al.* Epidermal growth factor and temperature regulate keratinocyte differentiation. *Arch. Dermatol. Res.* **289**, 317–326 (1997). doi: 10.1007/s004030050198
55. Mak, V. H. W. *et al.* Barrier Function of Human Keratinocyte Cultures Grown at the Air-Liquid Interface. *J. Invest. Dermatol.* **96**, 323–327 (1991). doi: 10.1111/1523-1747.ep12465212
56. Freshney, R. I. Biology of Cultured Cells. in *Culture of Animal Cells: A Manual of Basic Technique* (ed. Freshney, R. I.) 31–42 (John Wiley & Sons, 2005). doi:10.1002/0471747599.cac003
57. Freshney, R. I. Differentiation. in *Culture of Animal Cells: A Manual of Basic Technique* (ed. Freshney, R. I.) 281–290 (John Wiley & Sons, 2005). doi:10.1002/0471747599.cac003
58. Rosdy, M. & Clauss, L.-C. Terminal epidermal differentiation of human keratinocytes grown in chemically defined medium on inert filter substrates at the air-liquid interface. *J. Invest. Dermatol.* **95**, 409–414 (1990). doi: 10.1111/1523-1747.ep12555510
59. van der Valk, J. *et al.* Optimization of chemically defined cell culture media - Replacing fetal bovine serum in mammalian in vitro methods. *Toxicol. Vitro.* **24**, 1053–1063 (2010). doi: 10.1016/j.tiv.2010.03.016
60. Lamb, R. & Ambler, C. A. Keratinocytes Propagated in Serum-Free , Feeder-Free Culture Conditions Fail to Form Stratified Epidermis in a Reconstituted Skin Model. *PLoS One* **8**, e52494 (2013). doi: 10.1371/journal.pone.0052494
61. Watanabe, I. & Okada, S. Effects of temperature on growth rate of cultured mammalian cells (L5178Y). *J. Cell Biol.* **32**, 309–323 (1967). doi: 10.1083/jcb.32.2.309
62. Borowiec, A.-S., Delcourt, P., Dewailly, E. & Bidaux, G. Optimal Differentiation of In Vitro Keratinocytes Requires Multifactorial External Control. *PLoS One* **8**, e77507 (2013). doi: 10.1371/journal.pone.0077507
63. OECD. Test No. 428: Skin Absorption : In Vitro Method. in *OECD Guidelines for the Testing of Chemicals, Section 4* (OECD Publishing, 2004). doi:10.1787/9789264071087-en.
64. Goudar, C. *et al.* Applications of Quasi Real-Time Metabolic Flux Analysis in Mammalian Cell Culture Process Development. in *Animal Cell Technology meets Genomics* (eds. Gòdia, F. & Fussenegger, M.) 431–438 (Springer, 2005). doi:10.1007/1-4020-3103-3\_84
65. Place, T. L., Domann, F. E. & Case, A. J. Limitations of oxygen delivery to cells in culture: An underappreciated problem in basic and translational research. *Free Radic. Biol. Med.* **113**, 311–322 (2017). doi: 10.1016/j.freeradbiomed.2017.10.003
66. Evaristo, S. F. S. Metabolomic analysis of the reconstructed epidermis cultivation protocol as a tool to improve the skin barrier properties. (Tese de Mestrado em Biologia Humana e Ambiente; Faculdade de Ciências da Universidade de Lisboa, 2017).
67. Berg, J. M., Tymoczko, J. L., Gatto, G. J. & Stryer, L. *Biochemistry*. (W. H. Freeman and Company, 2015). doi:10.1360/zd-2013-43-6-1064
68. Ruela, A. L. M., Perissinato, A. G., Lino, M. E. de S., Mudrik, P. S. & Pereira, G. R. Evaluation of skin absorption of drugs from topical and transdermal formulations. *Brazilian J. Pharm. Sci.* **52**, 527–544 (2016). doi: 10.1590/s1984-82502016000300018

69. Finnin, B., Walters, K. A. & Franz, T. J. In Vitro Skin Permeation Methodology. in *Transdermal and Topical Drug Delivery: Principles and Practice* (eds. Benson, H. A. E. & Adam C. Watkinson) 85–108 (John Wiley & Sons, 2012). doi:10.1002/9781118140505.ch5
70. HarunRasheed, S. *et al.* Transdermal Drug Delivery System - Simplified Medication Regimen - A Review. *Res. J. Pharm. Biol. Chem. Sci.* **2**, 223–238 (2011).
71. Ng, S.-F., Rouse, J. J., Sanderson, F. D., Meidan, V. & Eccleston, G. M. Validation of a Static Franz Diffusion Cell System for In Vitro Permeation Studies. *AAPS PharmSciTech* **11**, 1432–1441 (2010). doi: 10.1208/s12249-010-9522-9
72. Cascade Biologics. Human Epidermal Keratinocytes, neonatal (HEKn) - Manual. (2009).
73. Kim, N., El-Khalili, M., Henary, M. M., Strekowski, L. & Michniak, B. B. Percutaneous penetration enhancement activity of aromatic S,S-dimethyliminiosulfuranes. *Int. J. Pharm.* **187**, 219–229 (1999). doi: 10.1016/S0378-5173(99)00194-5
74. Magnusson, B. M., Anissimov, Y. G., Cross, S. E. & Roberts, M. S. Molecular Size as the Main Determinant of Solute Maximum Flux Across the Skin. *J. Invest. Dermatol.* **122**, 993–999 (2004). doi: 10.1111/j.0022-202X.2004.22413.x
75. Cross, S. E., Anissimov, Y. G., Magnusson, B. M. & Roberts, M. S. Bovine-Serum-Albumin-Containing Receptor Phase Better Predicts Transdermal Absorption Parameters for Lipophilic Compounds. *J. Invest. Dermatol.* **120**, 589–591 (2003). doi: 10.1046/j.1523-1747.2003.12083.x
76. Thakkar, A. L. & Hall, N. A. Micellar Solubilization of Testosterone III: Dissolution Behavior of Testosterone in Aqueous Solutions of Selected Surfactants. *J. Pharm. Sci.* **58**, 68–71 (1969). doi: 10.1002/jps.2600580113
77. Netzlaff, F. *et al.* Permeability of the reconstructed human epidermis model Episkin® in comparison to various human skin preparations. *Eur. J. Pharm. Biopharm.* **66**, 127–134 (2007). doi: 10.1016/j.ejpb.2006.08.012
78. Zhang, Y.-Z. *et al.* Spectroscopic studies on the interaction of lanthanum ( III ) 2-oxo-propionic acid salicyloyl hydrazone complex with bovine serum. *Luminescence* **23**, 150–156 (2008). doi: 10.1002/bio.1025
79. Thermo Fisher Scientific. NanoDrop 2000 / 2000c Spectrophotometer - Manual. (2009).
80. Belay, A., Ture, K., Redi, M. & Asfaw, A. Measurement of caffeine in coffee beans with UV/vis spectrometer. *Food Chem.* **108**, 310–315 (2008). doi: 10.1016/j.foodchem.2007.10.024
81. Gallego, J. M. L. & Arroyo, J. P. Spectrophotometric determination of hydrocortisone, nystatin and oxytetracycline in synthetic and pharmaceutical preparations based on various univariate and multivariate methods. *Anal. Chim. Acta* **460**, 85–97 (2002). doi: 10.1016/S0003-2670(02)00138-1
82. He, W., Guo, X. & Zhang, M. Transdermal permeation enhancement of N-trimethyl chitosan for testosterone. *Int. J. Pharm.* **356**, 82–87 (2008).doi: 10.1016/j.ijpharm.2007.12.050
83. Brodin, B., Steffansen, B. & Nielsen, C. U. Passive diffusion of drug substances: the concepts of flux and permeability. in *Molecular Biopharmaceutics: Aspects of drug characterisation, drug delivery and dosage form evaluation* (eds. Steffansen, B., Brodin, B. & Nielsen, C. U.) 135–152 (Pharmaceutical Press, 2010).
84. Lichtenthaler, H. K. & Buschmann, C. Chlorophylls and Carotenoids: Measurement and Characterization by UV-VIS Spectroscopy. *Curr. Protoc. Food Anal. Chem.* **1**, F4.3.1-F4.3.8 (2001). doi: 10.1002/0471142913.faf0403s01
85. Systat Software Inc. SigmaStat 4.0. (2016).

86. Poumay, Y. *et al.* A simple reconstructed human epidermis: Preparation of the culture model and utilization in in vitro studies. *Arch. Dermatol. Res.* **296**, 203–211 (2004). doi: 10.1007/s00403-004-0507-y
87. Catarino, C. M. *et al.* Skin corrosion test: a comparison between reconstructed human epidermis and full thickness skin models. *Eur. J. Pharm. Biopharm.* **125**, 51–57 (2018). doi: 10.1016/j.ejpb.2018.01.002
88. Schäfer-Korting, M. *et al.* The use of reconstructed human epidermis for skin absorption testing: results of the validation study. *Altern. to Lab. Anim.* **36**, 161–187 (2008). doi: 10.1177/026119290603400312
89. Jean, J., Bernard, G., Duque-Fernandez, A., Auger, F. A. & Pouliot, R. Effects of Serum-Free Culture at the Air–Liquid Interface in a Human Tissue-Engineered Skin Substitute. *Tissue Eng. Part A* **17**, 877–888 (2011). doi: 10.1089/ten.tea.2010.0256

# APPENDIX A

## FRANZ CELL DIMENSIONS

### ○ Franz Cell No. 1

$\varnothing_{\text{donor (internal)}} = 14.36 \text{ mm}$

$\varnothing_{\text{receiver (internal)}} = 13.60 \text{ mm}$

$A_{\text{receiver (internal)}} = 145.2672 \text{ mm}^2$

$V_{\text{receiver}} = 13.90 \text{ mL}$

### ○ Franz Cell No. 2

$\varnothing_{\text{donor (internal)}} = 14.21 \text{ mm}$

$\varnothing_{\text{receiver (internal)}} = 13.59 \text{ mm}$

$A_{\text{receiver (internal)}} = 145.0537 \text{ mm}^2$

$V_{\text{receiver}} = 12.60 \text{ mL}$

### ○ Franz Cell No. 3

$\varnothing_{\text{donor (internal)}} = 13.86 \text{ mm}$

$\varnothing_{\text{receiver (internal)}} = 14.10 \text{ mm}$

$A_{\text{receiver (internal)}} = 156.1450 \text{ mm}^2$

$V_{\text{receiver}} = 13.20 \text{ mL}$

### ○ Franz Cell No. 4

$\varnothing_{\text{donor (internal)}} = 14.15 \text{ mm}$

$\varnothing_{\text{receiver (internal)}} = 13.81 \text{ mm}$

$A_{\text{receiver (internal)}} = 149.7881 \text{ mm}^2$

$V_{\text{receiver}} = 13.70 \text{ mL}$

### ○ Franz Cell No. 5

$\varnothing_{\text{donor (internal)}} = 14.43 \text{ mm}$

$\varnothing_{\text{receiver (internal)}} = 14.31 \text{ mm}$

$A_{\text{receiver (internal)}} = 160.8308 \text{ mm}^2$

$V_{\text{receiver}} = 14.30 \text{ mL}$

### Millicell Cell Culture Inserts

$\varnothing_{\text{internal}} = 10 \text{ mm}$

$A_{\text{insert}} = 0.7854 \text{ cm}^2$